People's Democratic Republic of Algeria
Ministry of Higher Education and Scientific Research

University M'Hamed BOUGARA – Boumerdes

Institute of Electrical and Electronic Engineering

Department of Power and Control

Final Year Project Report Presented in Partial Fulfilment of the Requirements for the Degree of

MASTER

In **Power Engineering**

Option: **Power Engineering**

Title:

Evaluation of Global MPPT for stand-alone PV System

Presented by:

- **SOUFI Ali**
- **MOHAMMADI Abdelhaq**

Supervisor:

Dr.Kheldoun Aissa

Registration Number:……/2018

Abstract

Under partial shading conditions (e.g., due to buildings, trees, and clouds), multiple peaks may exist on the power-voltage (P-V) characteristic curve of photovoltaic (PV) array, leading to the conventional maximum power point tracking methods fail to extract the global maximum power point (GMPP). To further complicate matters, most conventional Maximum Power Point Tracking methods develop errors under certain circumstances (for example, they detect the local Maximum Power Point (LMPP) instead of the global MPP) and reduce the efficiency of PV systems even further. Presently, much research has been undertaken to improve upon them. This work describes a new fast and efficient technique based on Particle Swarm Optimization (PSO), compared with the conventional technique Perturb and Observe (P&O) which is inadequate to track the GMPP subject to these conditions resulting in a dramatic reduction in the efficiency of the PV system.

Simulations are performed in MATLAB/SIMULINK software. A system includes a DC-DC buck-boost converter to step up or down the voltage to required magnitude. P&O and PSO maximum power point tracking (MPPT) algorithms have been used to extract the possible maximum power point from the PV system. A DSP microcontroller is also used to control the duty cycle of the IGBT accompanied with this system.

The results verify the accuracy of the proposed scheme. Also the results show that the proposed method has better characteristic and performance in compare with P&O methods.

Dedication

This work is dedicated to every individual who helped me walk through my path to succeed in this educational and academic journey, which was a long one filled with hard work and perseverance, the task wasn't easy like everything in life because success wasn't meant to be that way and for that sacrifices were to be made and struggles were to be endured, I would like thank my parents who took a major part in this course, even though thank you isn't enough to repay their favour for the reason that they gave everything they could to make the thing as easy as possible for me, I also want to express my deepest gratitude to the lovely people I met at my trainings who provided me all the knowledge they could. Finally, I would like send my greatest love to my sisters, friends and family members who were also a source for my aspirations ambitions.

MOHAMMADI Abdelhaq

I would like to dedicate this project to my beloved parents, my source of inspiration and the fuel that keeps me going. To my sister Imene who offered unlimited support and care. I would also like to thank my childhood friends whom I consider as brothers; Chakib, Houssam and Mimou. To the comrades who made my journey a lot more enjoyable. To the people who care about our well-being and success.

Finally, I would like to thank my partner, the best partner in the world; Hakou and everyone who contributed to the achievement of this work, and the ones who were there for me since the very beginning… Thank you.

SOUFI Ali

Acknowledgement

Writing this report has been fascinating and extremely rewarding. We would like to thank a number of people who have contributed to the result in many different ways.

To commence with, we pay our obeisance to Allah, the almighty to have bestowed upon us good health, courage and inspiration.

After Allah, we express our sincere and deepest gratitude to our supervisor, **Dr.KHELDOUN Aissa**, who ploughed through several preliminary versions of our text, making critical suggestions and posing challenging questions. His expertise, invaluable guidance, constant encouragement, understanding, patience and healthy criticism added considerably to our experience. Without his continual inspiration, it would have not been possible to complete this study.

We would like to express our gratitude to all IGEE teachers and staff for their kindness and great help they provide to us to finish this work, especially **Dr.Metidji Brahim** from whom we acquired very useful advices and guidance in fulfilling our work.

Finally, we must express our very profound gratitude to our parents and family for providing us with unfailing support and continuous encouragement throughout our years of study and through the process of researching and writing this report. This accomplishment would not have been possible without them. Thank you.

Table of contents:

List of tables

List of Figures

Abbreviations

AC	Alternative current
DC	Direct current
ESR	Electrical service requirement
I	Current [A]
I_{pv}	Photovoltaic current [A]
I_{0}	Saturation current [A]
I_{mpp}	Maximum power point current [A]
GMPPT	Global maximum power point tracking
LMPPT	Local maximum power point tracking
I_{sc}	Short circuit current [A]
G	Irradiance [w/m^2]
Gbest	Global best
MPP	Maximum power point
MPPT	Maximum power point tracking
N_s	Number of series connected cells
RMS	Root mean square
STC	Standard temperature condition
Si	Silicon
P	Power [W]
Pbest	Personal best
P&O	Perturb and observe
PSO	Particle swarm optimization
PV	Photovoltaic
PVG	Photovoltaic generator
PWM	Pulse width modulation
T	Temperature [C°]

V	Voltage [V]
V_{pv}	Photovoltaic voltage [V]
V_{oc}	Open circuit voltage [V]
V_{mpp}	Maximum power point voltage [V]

General Introduction

General introduction

Electric Energy is considered to be the driving force in contemporary life and economy. Since the industrial revolution, energy demand has greatly increased, not only in the western world, but all over the world. As a result, two problems emerged: first, energy crisis and more recently climate change (global warming). Therefore, the sustainability of our civilization is seriously threatened by the world widely energy demand and gas emissions from greenhouses. It is a global challenge to tackle climate change by reducing carbon dioxide emissions and ensuring secure, clean and affordable energy. One possible solution to achieve more sustainable energy systems is to use the environment-friendly energy sources such as "Solar Energy ".

Photovoltaic technology is used to describe the hardware made of semiconductor materials, which converts sunlight into electrical power. The photovoltaic modules that perform this conversion have many benefits. They are durable, reliable, minimal maintenance requirement, completely silent and require only sunlight as fuel. However, their high dependence to weather conditions (temperature and irradiance) and relatively low conversion efficiency are their main drawbacks.

The efficiency of a PV plant is principally affected by three agents: the PV panel’s efficiency, the converter’s efficiency and the MPPT algorithm’s efficiency. Improving the efficiencies of the PV panel or the converter is not an easy task due to the available technology limitations. Instead, improving the tracking of the (MPP) with more reliable control algorithms is possible, not expensive and can be applied even in plants which are already in service just by updating their MPPT control algorithms.

In fact, several MPPT methods which vary in complexity, convergence speed, cost, range of effectiveness and implementation hardware have been proposed. Most of them are DC/DC chopper circuits based such as perturb and observe (P&O) and particle and swarm (PSO) methods, assimilate different MPPT strategies and give some general reviews over them.

The main aim of this work is to develop a new MPPT method using particle and swarm (PSO) algorithm. This technique will be studied, analyzed then compared with results of perturb and observe (P&O) algorithm, to verify its benefits. Furthermore, a hardware prototype will be designed and implemented based on DSP microcontroller dedicated to test the developed algorithm using real environmental conditions.

Chapter One:

Modeling of PV Generator

1. Introduction

A Photovoltaic system converts sunlight into electricity. It can be generally divided into two basic groups; stand-alone and grid connected PV systems. Solar cells are the fundamental devices of a PV system. To increase the amount of power produced by this system, solar cells may be grouped together to form modules that may be connected in series or in parallel to form an array. In this chapter, the basic operation of solar cells and structure will be introduced in details, along with mathematical model of it. Also, some factors that affect the operation of PV cells are discussed [1].

2. PV cell

A photovoltaic cell is basically a semiconductor diode whose p– n junction is exposed to light. Photovoltaic cells are made of several types of semiconductors using different manufacturing processes. The monocrystalline and polycrystalline silicon cells are among technologies found at commercial scale at the present time.

Silicon PV cells are composed of a thin layer of bulk Si or a thin Si film connected to electric terminals. One of the sides of the Si layer is doped to form the p– n junction. A thin metallic grid is placed on the Sun-facing surface of the semiconductor.

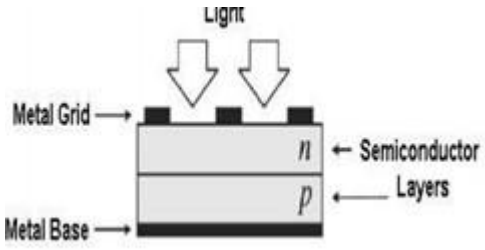

Figure 1.1: p-n junction of PV cell

The incidence of light on the cell generates charge carriers that originate an electric current if the cell is short circuited. Charges are generated when the energy of the incident photon is sufficient to detach the covalent electrons of the semiconductor, this phenomenon depends on the semiconductor material and on the wavelength of the incident light. Figure 1.2 shows the equivalent circuit of the PV cell model. It consists of a photocurrent, a diode, a parallel resistor expressing a leakage current, and a series resistor describing an internal resistance to the current flow [1].

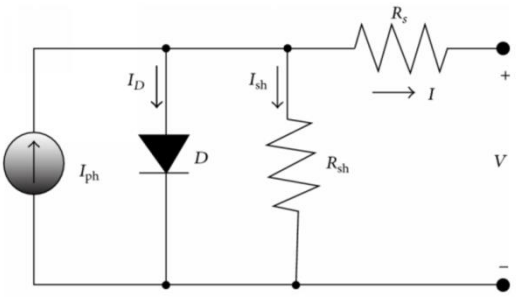

Figure 1.2: Equivalent model pf PV cell

The V − I characteristic equation of a solar cell is given as:

$$I = \left(I_{ph} - I_0 * \left(e^{(V+I*R_s)*\frac{1}{a*Vt}} - 1\right) - \frac{V-I*R_s}{R_p}\right) \text{.....1.1}$$

Where

I_{ph}: is a light generated photon current,

I_0: cell saturation of dark current,

R_p: Shunt resistance in Ω,

R_s: Series resistance in Ω,

***a*:** Ideality factor [1.6 for silicon].

Photon current is the current in the cell that results from solar radiation. It depends on both the temperature and irradiance, therefore, its value stays constant regardless the external voltage. It is given by the following equation:

$$I_{ph} = \frac{G}{G_n} * \left(I_{phn} + K_i * (T - T_n)\right) \text{.....1.2}$$

Where

I_{phn}: nominal photon current at STC,

T: cell temperature in Kelvin,

T_n: nominal temperature in Kelvin at STC, 25°C,

K_i: Short circuit current temperature coefficient,

G: Solar irradiation in 1 kW/m2,

G_n : Solar irradiation in KW/m2.

Cell saturation current is the reverse diode saturation current, it depends only on the temperature, and it can be calculated using:

$$I_0 = \frac{I_{scn} + K_i \times (T - T_n)}{e^{\frac{V_{ocn} + K_v \times (T - T_n)}{a \times V_t}} - 1} \quad \text{.....1.3}$$

Where

I_{scn}: is the nominal short circuit current at STC,

V_{ocn}: is the nominal open circuit voltage at STC,

K_v: open circuit voltage temperature coefficient at Isc.

thermal voltage is given by:

$$V_t = \frac{K \times T}{q} \quad \text{.....1.4}$$

Where

K: Boltzmann's constant 1.38×10^{-23} J/K,

q: is the charge of electron 1.6×10^{-19} C.

3. PV module

Since an individual cell produces only about 0.6V, it is a rare application for which just a single cell is of any use. Instead, the basic building block for PV applications is a module consisting of a number of pre-wired cells in series, all encased in tough, weather-resistant packages. A typical module has 36 cells in series and is often designated as a "12-V module" even though it is capable of delivering much higher voltages than that. Large 72-cell modules are now quite common, some of which have all of the cells wired in

series, in which case they are referred to as 24-V modules [2]. The following equation characterized its I – V relations:

$$I = (I_{ph} - I_0 \times \left(e^{(v+I\times R_S)\times\frac{1}{a*V_t*N_S}} - 1\right) - \frac{V-I\times R_S}{R_p} \quad \text{.....1.5}$$

Where: N_s is the number of cells, usually 36, 72… etc.

4. PV array

A PV array is set of PV module, that can be wired in series to increase voltage, and in parallel to increase current. Arrays are made up of some combination of series and parallel modules to increase power.

For modules in series, the I – V curves are simply added along the voltage axis; as shown in figure 1.3. That is, at any given current (which flows through each of the modules), the total voltage is just the sum of the individual module voltages.

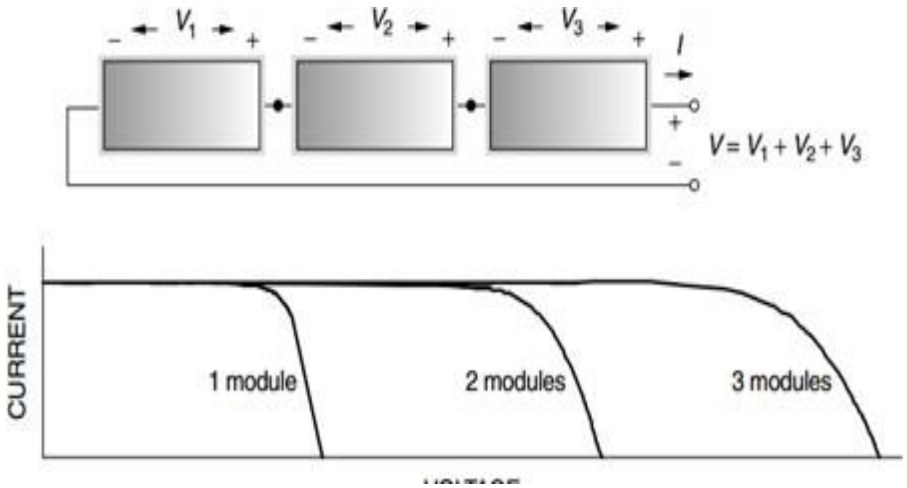

Figure 1.3: PV modules connected in series

For modules in parallel, the same voltage is across each module and the total current is the sum of the currents. That is, at any given voltage, the I – V curve of the parallel combination is just the sum of the individual module currents at that voltage.

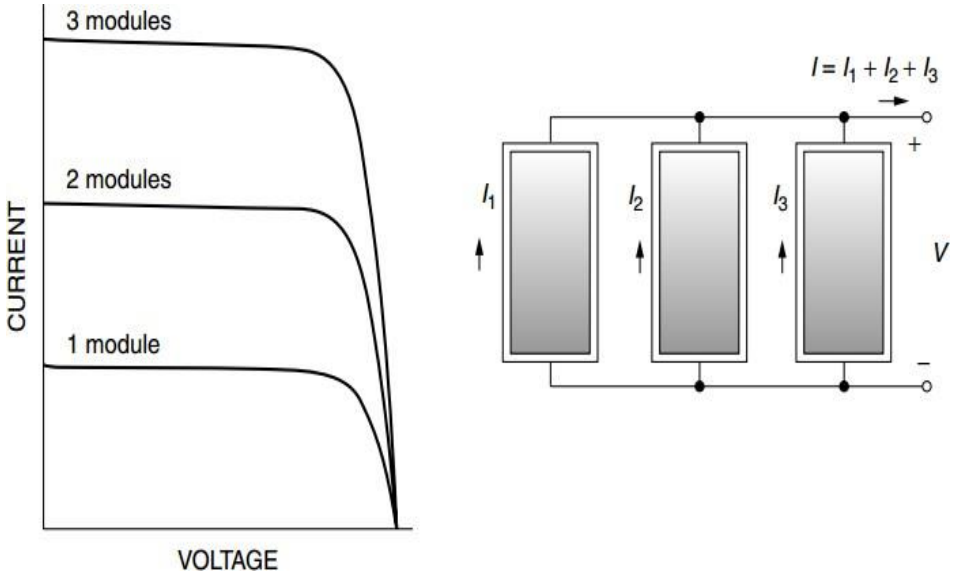

Figure 1.4: PV modules connected in parallel

When high power is needed, the array will usually consist of a combination of series and parallel modules for which the total I – V curve is the sum of the individual module I – V curves [3].

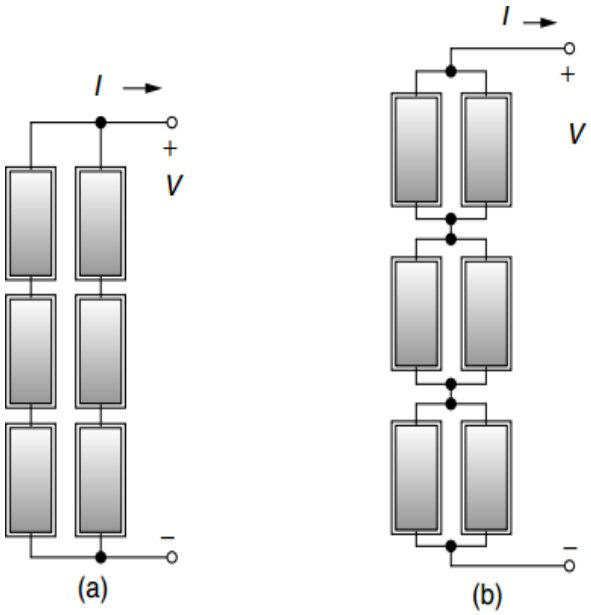

Figure 1.5: Different connection for parallel/series PV array

The mathematical model for the PV array is expressed by :

$$I = \left(N_{PP} I_{ph} - N_{pp} I_0 \times \left(e^{\left(\frac{V}{N_s} + \frac{I}{N_{pp}} \times R_s\right) \times \frac{1}{a \times V_t \times N_s}} - 1 \right) - \frac{V \times \frac{N_{ss}}{N_{pp}} - I \times R_s}{R_p} \right) \text{.....1.6}$$

Where:

N_{pp}**:** is the number of module connected in parallel.

$\mathbf{N_{ss}}$**:** is the number of module connected in series.

5. Power loss in PV module

One of the few disadvantages of using PV modules is its low efficiency, which is approximately equal to 16% . There are multiple reasons for this power loss which are:

- Top surface contact obstruction, loss around 3%.
- Reflection at top surface, loss around 1%.
- Photon energy less than band gap, loss around 20.2%.
- Excess photon energy, loss around 33%.
- Voltage factor F_v, loss around 20% .
- Fill factor F_c, loss around 4%.
- Ideality factor “a”, loss around 3%.
- Series resistance, loss around 0.3%.
- Shunt resistance, loss around 0.1%.

6. Effect of temperature and irradiance on the I-V characteristics

Temperature is another factor which shows a momentous influence on the characteristic of solar cell. Figure 1.6 shows that with the increase in temperature open circuit voltage increases proportionally but the short circuit current decreases logarithmically.

Figure 1.6 reflects this peculiarity of solar cell characteristic for different temperature values.

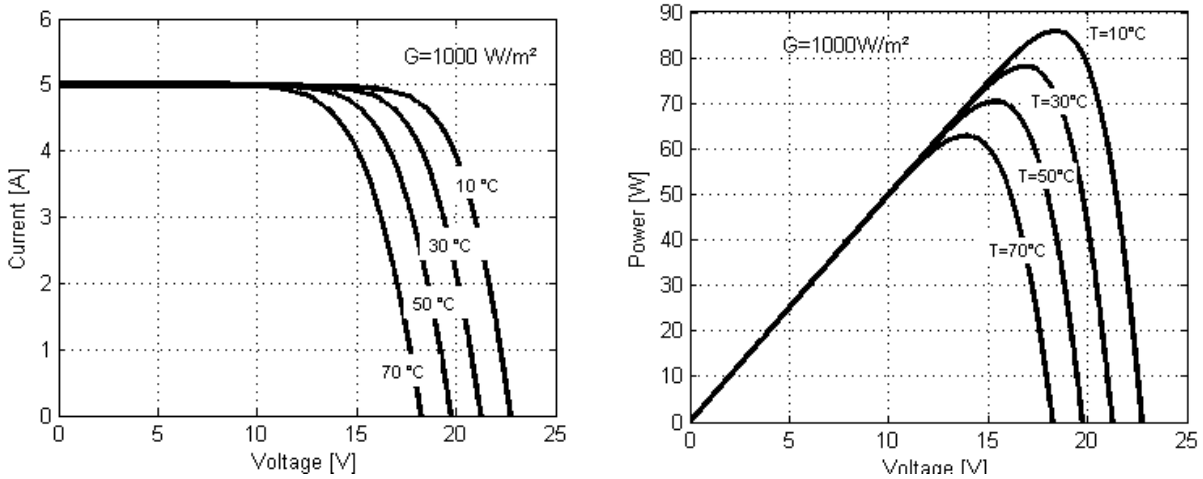

Figure 1.6: effect of temperature on I – V and P – V curves

The changes in characteristic with variation in insolation are shown in figure 1.7. The short circuit current (Isc) of the solar cell is the function of insolation and reduces proportionally with decrease in insolation.

Figure 1.7 reflects that the point of maximum power also varies with respect to changing insolation [4].

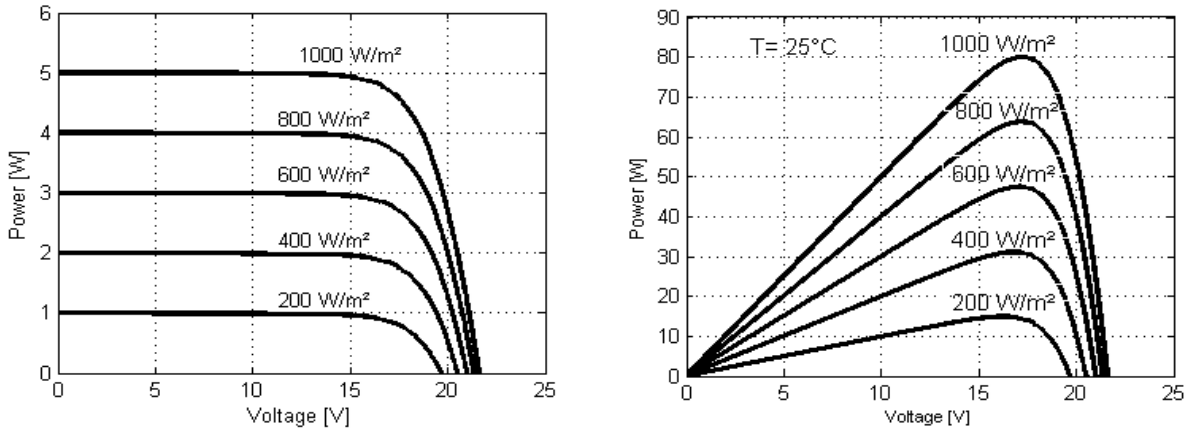

Figure 1.7: Effect of irradiance on I – V and P – V curves

7. Partial shading effect

Along with temperature and insolation partial shading also shows a major influence on solar cell characteristic. A PV array are shaded by a nearby tree, chimney, or cloud or….etc.

7.1. Effect of shading on PV module

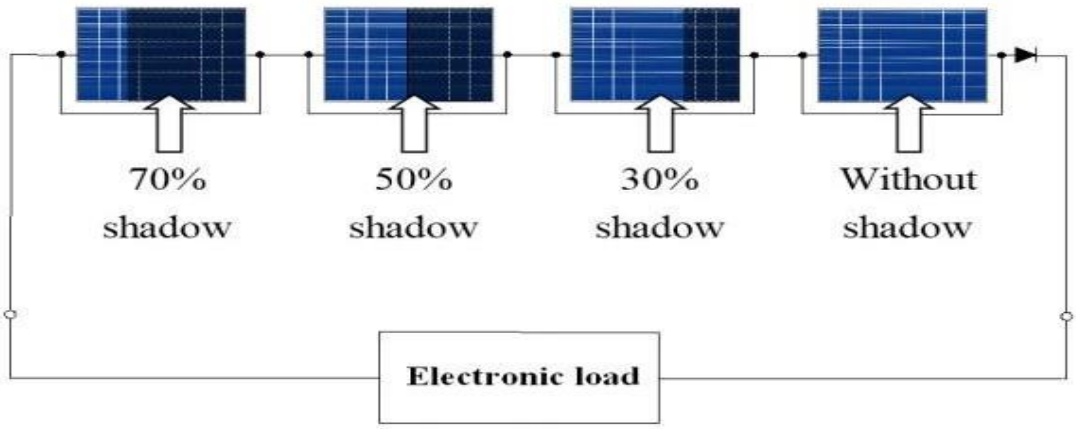

Figure 1.8: PV array with shaded modules

The output voltage of a PV cell is quite low (almost 0.6 V), to increase the output voltage a string of series connected PV cells is needed. Meanwhile, if a part of the string is shaded, the voltage generated by the shaded cells will be lower than that generated by unshaded cells, which results in the consumption of a part of the generated power by shaded cells.

In order to calculate the exact voltage drop in a PV module, we considered the following:

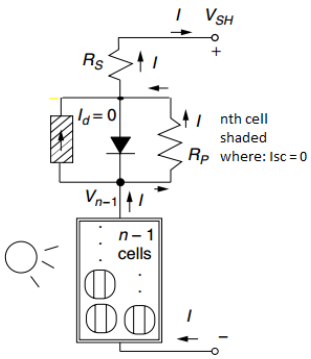

Figure 1.9: Equivalent circuit of PV module with a single shaded cell

$V_{sh} = V_{n-1}$-$(R_p+R_s)I$ 1.7

Where: V_{sh} is the voltage of the shaded cell

We can write the voltage of $(n-1)$ un-shaded cell as :

$$V_{n-1} = \left(\frac{n-1}{n}\right)V \text{.....1.8}$$

Where: n is the number of cells and V is the output voltage.

replacing 1.8 in 1.7 we get:

$$V_{sh} = \left(\frac{n-1}{n}\right)V - (R_P - R_s)I \text{ .....1.9}$$

Using the above equation, we can calculate the voltage drop for a single shaded cell by:

$$\Delta V = V - V_{sh} = V - \left[\left(\frac{n-1}{n}\right)V * (R_P + R_s)I\right] \text{ .....1.10}$$

$$\Delta V = \frac{V}{n} + \left(R_p + R_s\right)I \text{ .....1.11}$$

The partial shading not only results in significant power loss in the PV array, but also causes hot spots in the location of shaded cells, consequently reducing the lifetime of PV cells [5].

7.2. PV array protection

In order to ensure a long life for PVG , and avoid destructive faults of them, it is necessary to add some protection which often are blocking diodes and bypass diodes valves.

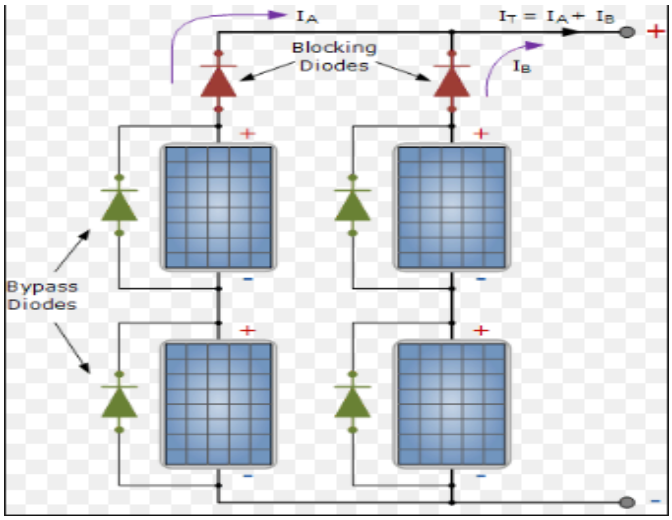

Figure 1.10: PV array protection

7-2-1-Blocking diode

Under the effect of the sun when the voltage produced by PVG is greater than that of the battery, the battery is charging. However, when darkness takes place, no voltage is produced by the PVG. Therefore, battery voltage causes a current which will flow in the reverse direction through the panels which can lead to the destruction of PVG. Hence the use of non-return (blocking) diodes will beneficial to block the passing current and protect the PVG.

7-2-2-Bypass diode

The bypass diode is connected in parallel but in opposite polarity to a PV cell. In normal operation, each solar cell is forward biased and therefore the bypass diode will be reverse biased and acts as an open circuit. However, a cell is polarized inversely due to a short-circuit between the cells, the bypass diode conduct when the current pass from solar cells to the external circuits [6].

8. Conclusion

In this chapter, we observed the effect of temperature and irradiance on the characteristics of the PV cells and modules. Some factors of which result power losses In a PVG cells were listed, and we discussed one major factor is partial shading. Also, we saw how to protect solar cells against this shading effect.

Chapter Two:

Maximum Power Point Tracking

1. Introduction

The Maximum Power Point Tracking (MPPT) is a technique used in power electronic circuits to extract maximum energy from the Photovoltaic (PV) Systems. However, because of the non-linear I–V characteristics of the PV curve that depends on the solar irradiance, cell temperature and output voltage of PV module, tracking the correct maximum power point (MPP) can sometimes be a challenging task. This chapter steps through a brief introduction to the conventional MPPT algorithm, such as Perturb and Observe. This technique is usually trapped at one of the local peak, simply because its algorithm could not distinguish between the local and global peaks. Also, a new method called Partial Swarm Optimization (PSO) which is well suited to cater for the partial shading conditions. Finally, ends up with a short comparison between them [7].

2. Maximum power point tracking theory

When a load is directly connected to the solar panel, the operating point of the panel will rarely be at the maximum power point. The distinct loads derive the operating point of the solar panel. Figure 2.1 shows the load lines of three unequal resistances and, the operating points are respectively A, B and C, the intersection between load lines and the I-V characteristic curve.

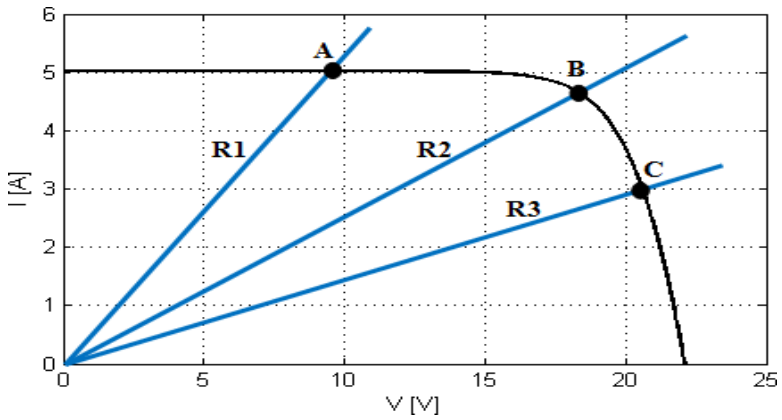

Figure 2.1: I-V curve with different operating points.

The operating point can be moved towards the MPP by varying the impedance seen by the panel. Since panels are DC devices, DC-DC converters must be utilized to transform the impedance of one circuit (source) to the other circuit (load). The I-V curve of the panel changes with the variation of the atmospheric conditions such as irradiance and temperature. Therefore, it is not feasible to fix the duty ratio with such dynamically changing operating conditions but utilize algorithms that frequently sample panel voltages and currents, and then adjust the duty ratio as needed.

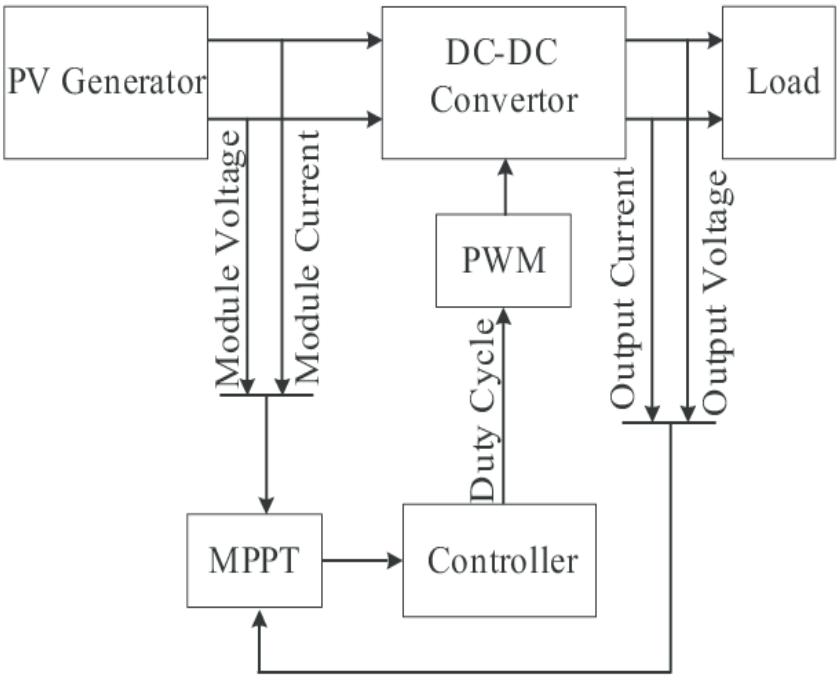

Figure 2.2: Detailed block diagram of stand-alone PV system.

3. Classical maximum power point tracking algorithms

3.1. Perturb and observe (P&O)

The Perturb and Observe method (P&O), sometimes called Hill climbing method, is the most famous MPPT technique. As the name of the P&O method states, the process starts by operating the DC-DC converter with the initial set duty cycle, and then starts increasing the duty cycle with a certain step width (user defined), and the power is

observed with the addition of each step. If at a certain point the power gets less than its previous value that means that the duty cycle should get one step in the opposite direction i.e. getting to the MPP again and etc… (See Figure 2.3). This algorithm is not appropriate in high variation of the solar irradiation. The voltage oscillates around the maximum power point and never reaches a precise value [8].

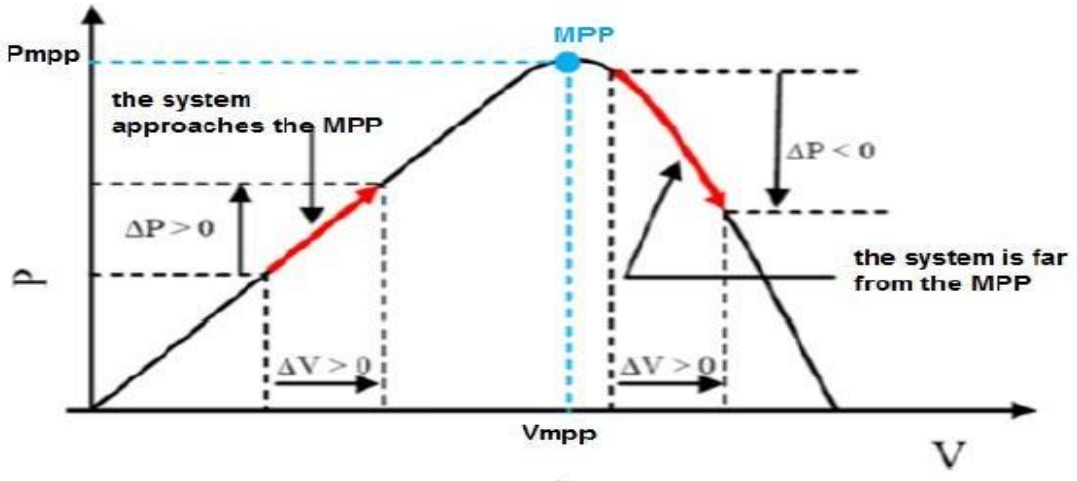

Figure 2.3: MPP search using P&O.

The different steps of the Perturb and Observe method are summarized as follow:

- Take current and voltage measurements.
- Calculate the power corresponding to the pervious measurements.
- If the power is constant, return to take new measurements, if the power decreased or increased, test the voltage variation.
- According to the direction of the voltage variation, modify the current duty cycle.

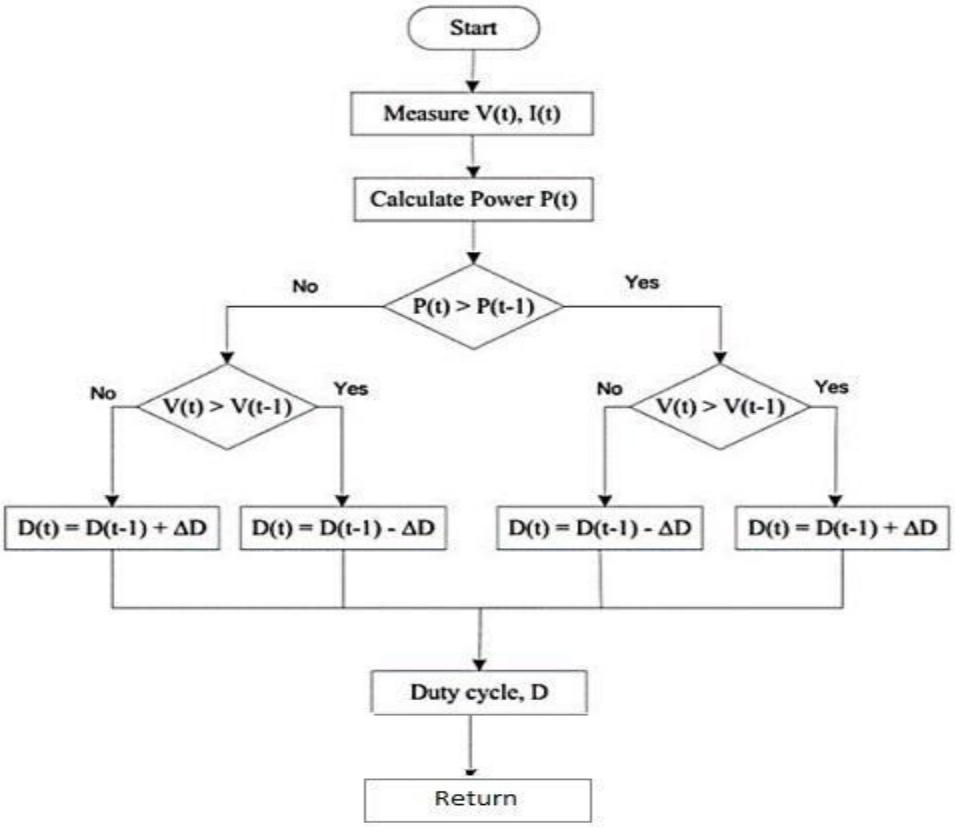

Figure 2.4: Flow chart of P and O algorithm.

4. Modern maximum power point tracking algorithms

4.1. Particle swarm optimization

4.1.1. Definition of PSO

Particle swarm optimization (PSO) algorithm is a population-based search method, proposed in 1995 by James Kennedy and Russell Eberhard to optimize nonlinear functions. It is inspired by the social behavior of organism such as birds flocking, fish schooling and bee swarming while searching for food, that individuals communicate in such a way that the entire population migrates toward the same target along the same direction.


Figure 2.5: Illustration of behavior of birds and fish.

Particle swarm optimization (PSO) algorithm consists of "n" particles, where each particle represents a candidate solution. Particles follow a simple behavior: emulate the success of neighboring particles, and achieve their own successes. The position of a particle is therefore influenced by the best particle solution in a neighborhood, as well as its best solution.

Each particle can be shown by its instantaneous speed and position, the most optimist position of each individual and the most optimist position of the surrounding. In PSO, the speed and position of each particle change according to the following equality [9]:

$$V_i^{k+1} = \omega V_i^k + c_1 r_1 \left(P_i^k - X_i^k\right) + c_2 r_2 \left(P_g^k - X_i^k\right) \quad \text{.....2.1}$$

$$X_i^{k+1} = X_i^k + V_i^{k+1} \quad \text{.....2.2}$$

In the formula:

i : is the ordinal number of particle.

k : presents the number of iteration.

V_i^k : is the velocity of the i^{th} particle at current moment.

V_i^{k+1} : is the velocity of the i^{th} particle at the next moment.

X_i^k : is the position of the i^{th} particle at current moment.

X_i^{k+1} : is the position of the i^{th} particle at the next moment.

P_i^k : is the individual best position of the i^{th} particle.

P_g^k : is the global best position.

ω : is the inertia weight.

c_1, c_2: are acceleration factor.

r_1, $r_2 \in (0, 1)$: are two independent random numbers.

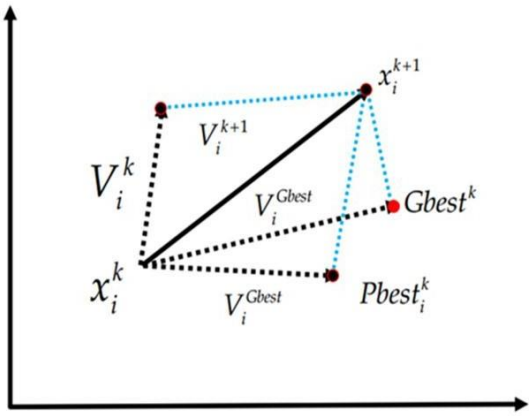

Figure 2.6: Position update using PSO

4.1.2. Steps of PSO algorithm

The fundamental PSO calculation can be clarified in five stages:

- Step 1: Initialization of the molecule position and speed arbitrarily.
- Step 2: Objective function assessment.
- Step 3: P_{best} and G_{best} assessment.
- Step 4: Updating of the speed and position.
- Step 5: Repetition of steps 2–4 until the criteria are met

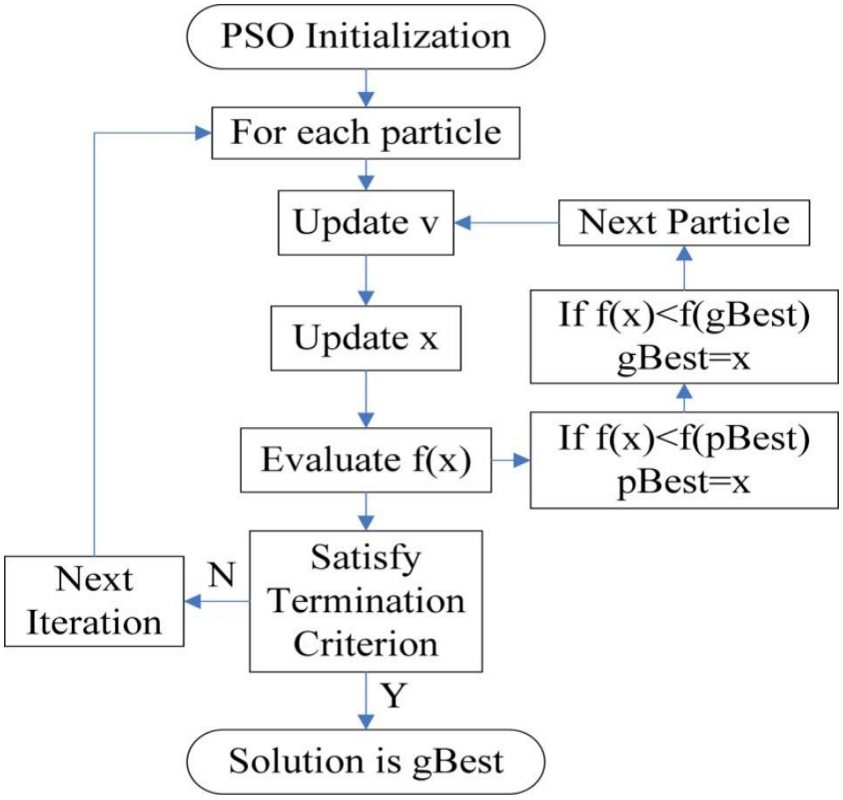

Figure 2.7: Flowchart of PSO algorithm4.2. PSO based MPPT.

4.2.1. Its principle

In order to find the MPP quickly, and to overcome the problems posed by conventional MPPT algorithms, speed, stability and accuracy, a novel maximum power point tracking controller based on Particle swarm optimization has been proposed.

Since partially shaded I–V curve exhibits multi peaks characteristics, PSO method is very effective to track the global point (GP) under this condition.

The complete flowchart for the proposed method is shown in figure 2.8 and the proposed algorithm uses the following basic principles [10]:

- **Step 1.** Parameter selection: For the proposed MPPT algorithm, the calculated duty cycle of the converter is defined as the particle position, the velocity defines the duty cycle incrementation and PV module output power is chosen as the fitness function.

- **Step 2.** PSO initialization: In a standard initialization, PSO particles are usually randomly initialized. For the proposed MPPT algorithm, the particles are initialized at fixed, equidistant points, within the predefined interval [0 - V_{oc}].

- **Step 3.** Fitness evaluation: The fitness evaluation of particle "i" will be conducted after the digital controller sends the PWM command according to the duty cycle, which also represents the position of particle "i".

- **Step 4.** Determination of individual and global best fitness: The new calculated individual best fitness (P_{best}) and the global best fitness (G_{best}) of each particle value are compared with previous ones. They are then replaced according to their positions, where necessary.

- **Step 5.** Updating the velocity and position of each particle: The velocity and position of each particle in the swarm is updated according to equations 2.1 and 2.2.

- **Step 6.** Convergence determination: The convergence criterion is checked. If the end criterion is met, the computation will terminate. Otherwise, the iteration is increased by one rerun of Steps 2 through 6.

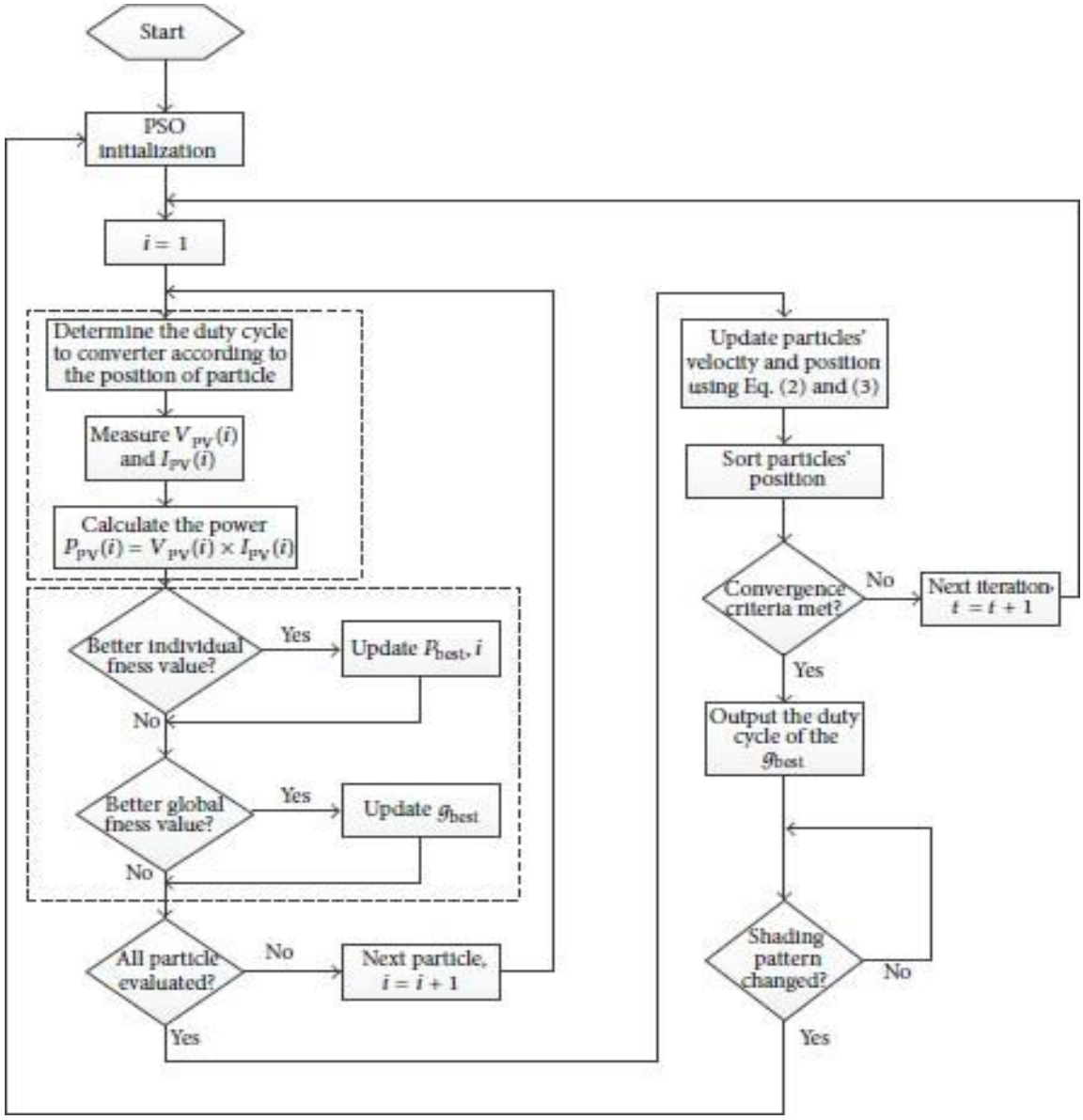

Figure 2.8: Flowchart of PSO based on MPPT.

4.2.2. The advantages of PSO

1. In the case of partial shading, the P-V curve is characterized by several peaks -depending on the environmental change. Hence, the PSO algorithm can track the global peak correctly unlike the conventional methods.

2. The individual best position and the global one are tracked at the same time, resulting a faster convergence.

3. Once the MPPT is reached the velocity of particles is zero, so there is no update in the duty cycle values, hence no oscillation will be seen at the steady state of the P-V curve [11].

5. DC-DC buck-boost converter

As we have seen, the MPPT algorithms cannot be implemented without using choppers. This makes the chopper the central stage in photovoltaic systems.

5.1. Equivalent circuit of the buck-boost converter

A buck-boost converter is the front-end component of a PV system connected between a PV array and a load. The dc-dc buck-boost converter has an output voltage magnitude that is either greater than or less than the input voltage magnitude. In this work we have chosen an inverting converter, the output voltage is of the opposite polarity than the input and it's adjustable based on the duty cycle of the switching transistor. The basic dc-dc buck-boost converter topology is shown in figure 2.9. It consists of two switches, one controlled (MOSFET, IGBT...) and one uncontrolled (diode), to achieve unidirectional power flow from the input to the output. This circuit, also, uses two capacitors and one inductor to store and transfer energy from input to output. They also, filter or smooth voltage and current [12].

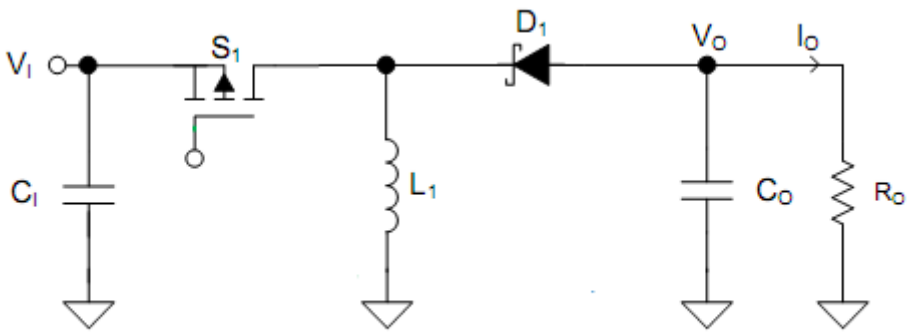

Figure 2.9: Simplified Schematic of an Inverting Buck-Boost Stage.

6. Conclusion

In this chapter, the principal of MPPT technique applied to photovoltaic (PV) power system was illustrated where MPPT techniques have been classified into two categories: conventional (P&O) and intelligent (PSO) methods. The flowchart of each method has been explained and discussed. We have also seen the advantage and disadvantage for each one of the different techniques.

Chapter Three:

Simulation and Results

1. Introduction

As mentioned before, we used SIMULINK to design and implement our circuit in the following parts, we will present our model for a simple stand-alone PV system. Also, we will compare and discuss two different algorithms used for tracking the maximum power in both normal and shaded conditions.

2. Overall system

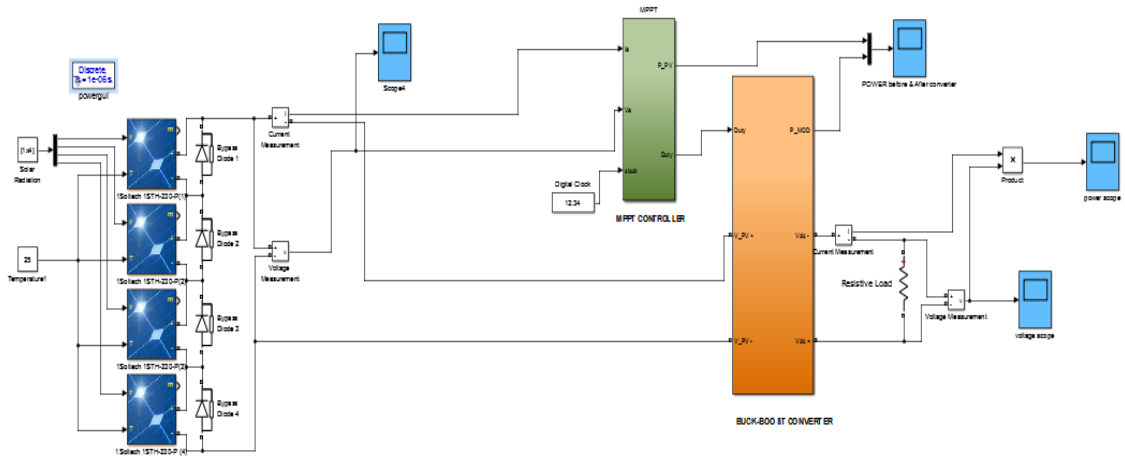

Figure 3.1: SIMULINK model of the overall system.

2.1. Calculation of the chopper parameters

The DC-DC buck-boost converter parameters are calculated using specific equations and assumptions (see appendix A), we summarized the required parameter of our system in the table 3.1.

Table 3.1: buck-boost converter parameters.

$f_{(sw)}$	Rload	L1	C_1	C_o
10 kHz	30Ω	47µH	2mF	2mF

3.PV Generator

3.1. Design

Figure.3.2 shows the equivalent circuit of the PV generator.

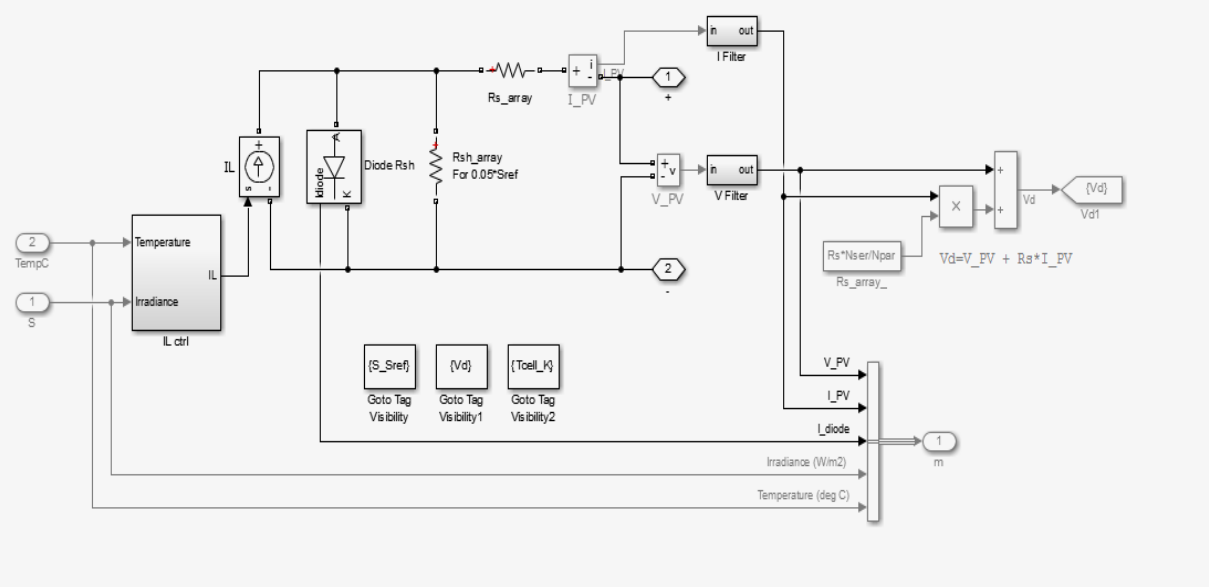

Figure 3.2: SIMULINK model for the equivalent circuit of PV generator.

In this work, we have chosen1Soltech 1STH-230-P panel for our simulation. The table below shows the parameters for this particular panel.

Table 3.2:1Soltech 1STH-230-P PV panel parameters.

I_{SC}	I_{mpp}	V_{OC}	V_{mpp}	P_{max}	K_i	k_V	N_s	T_n	G_n
8.18 (A)	7.65 (A)	37.1 (V)	29.9 (V)	228.7 (W)	0.102 (%/C °)	0.361 (%/C°)	60	25 (°C)	1000 ($W/m^{2)}$

The PV panel model design using Simulink is shown in the figure 3.3.

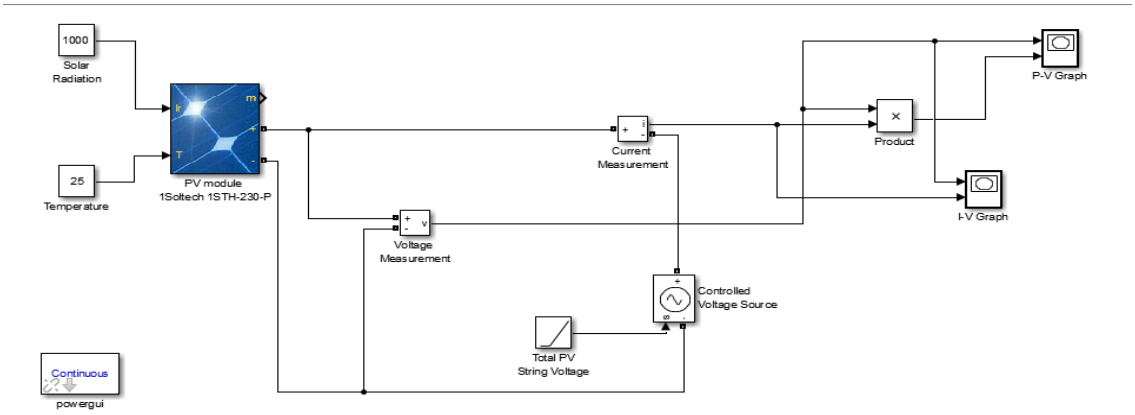

Figure 3.3: SIMULINK model for a single PV module.

The characteristic curves of the PV module obtained from the simulation are shown in figure 3.4:

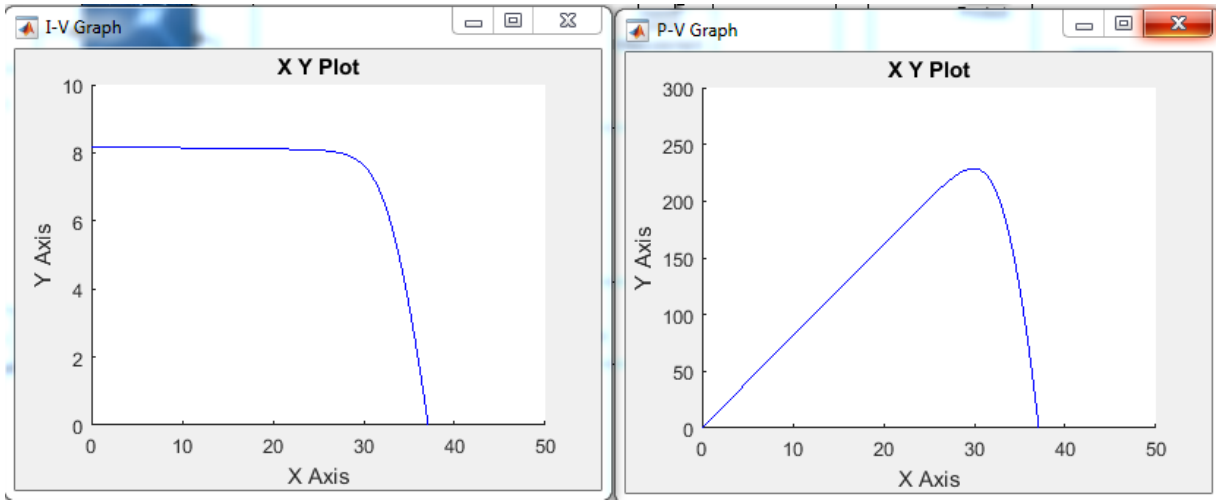

Figure 3.4: IV and PV curves of single module in uniform condition.

We connected multiple modules in series to create a PV array in order increase the voltage, which leads to an increase in the power.

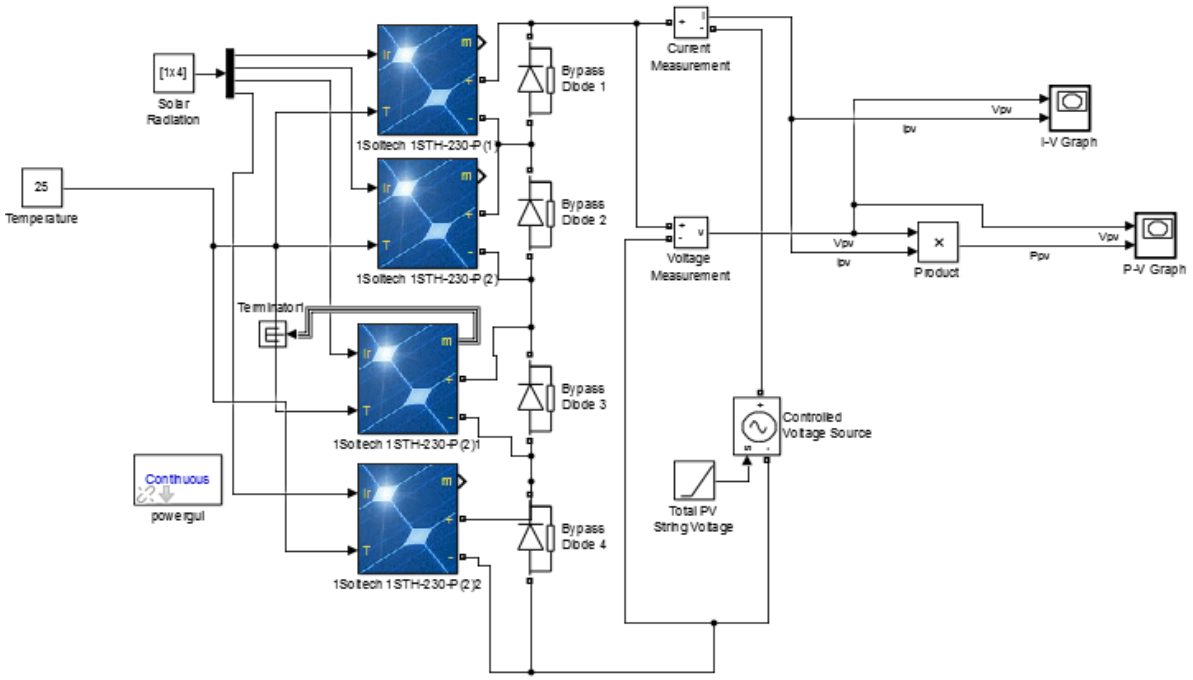

Figure 3.5: SIMULINK model for 4series connected modules in uniform condition.

The resulting IV and PV curves for the four (4) series module in uniform condition are show infigure3.6.

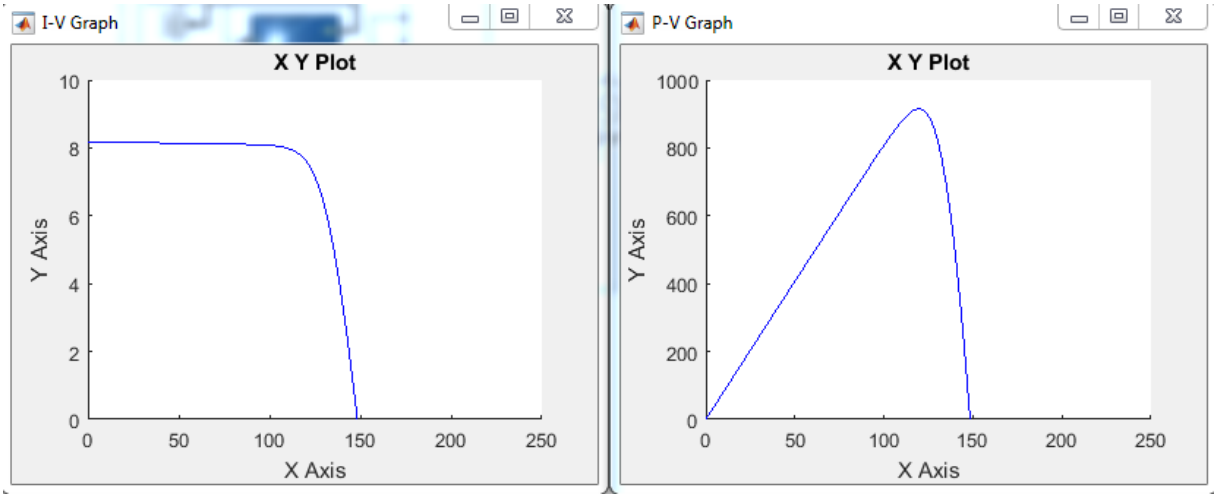

Figure 3.6: IV and PV curves for 4series connected modules in uniform condition.

3-2-Partial Shading

In this part, we used a simple circuit to observe the effect of protection diode under shading effect.

We used different irradiance values to illustrate this phenomenon, where one module at full sun (1000 W/m²) and the others are 800 W/m^2, 500W/m^2 and 300 W/m^{2}shaded.

3-2-1-Effect of bypass diode

We connected three PV modules in series without adding the bypass diodes.

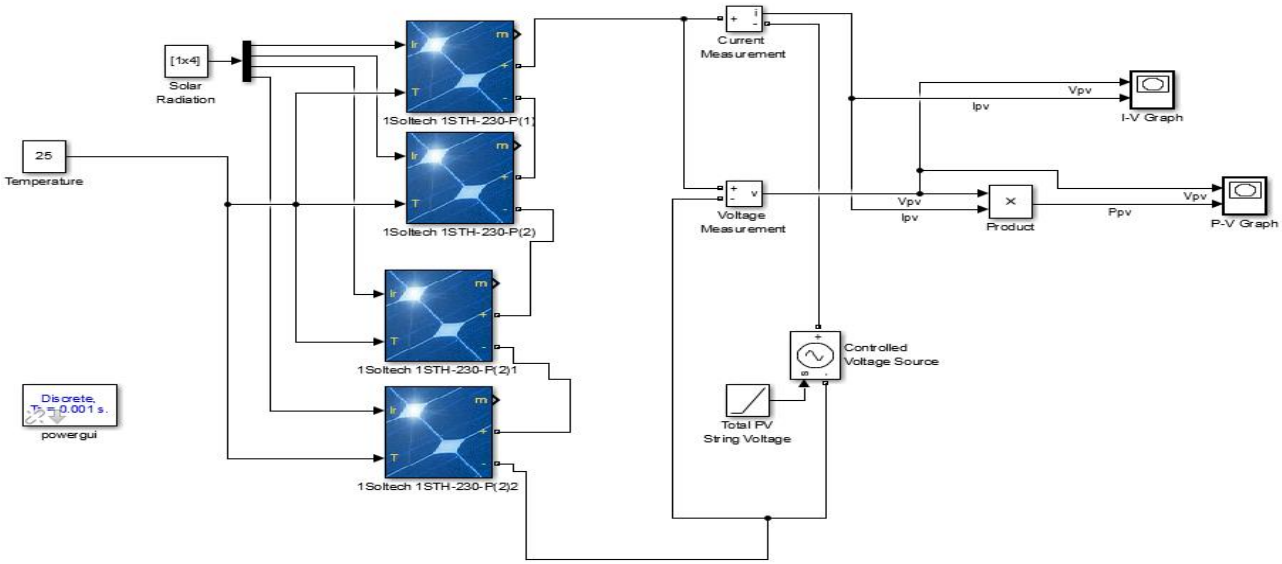

Figure 3.7: SIMULINK model for 4series connected modules in PSC without protection.

After running the simulation, we got the curves shown in figure 3.8.

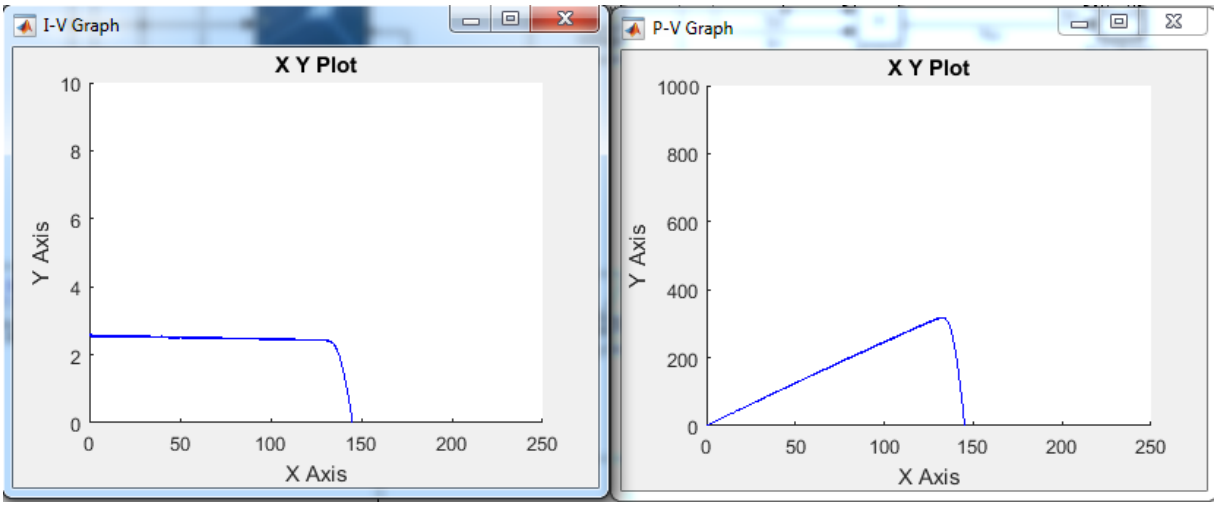

Figure 3.8: I-V and P-V curves model for 4 series connected modules in PSC without bypass diode.

After that we connected a bypass diode in parallel with each PV module as it is shown in figure 3.9.

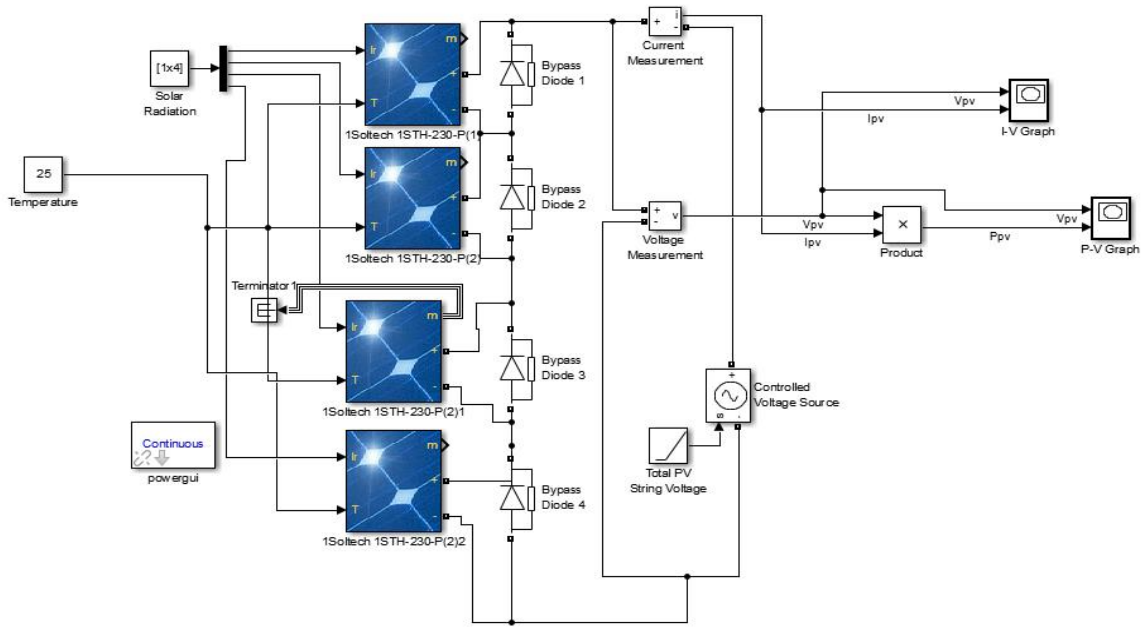

Figure 3.9: SIMULINK model for 4 series connected modules in PSC with protection.

After running the simulation, we got the curves shown in figure 3.10.

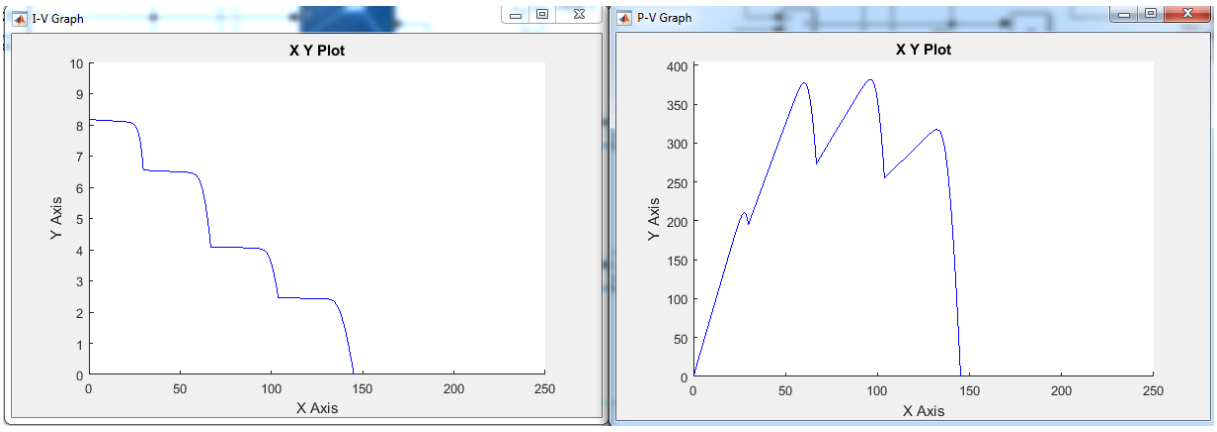

Figure 3.10: I-V and P-V curves model for 4 series connected modules under PSC.

4. MPPT controller

In the previous chapter, we discussed the theoretical part of MPP tracking and talked about some algorithms that can be used to do so. In this part, we will show the

difference between the selected methods, and discuss the results.

4.1. Design of the buck-boost DC-DC converter

First we design our buck-boost DC-DC converter using MATLAB-SIMULINK.

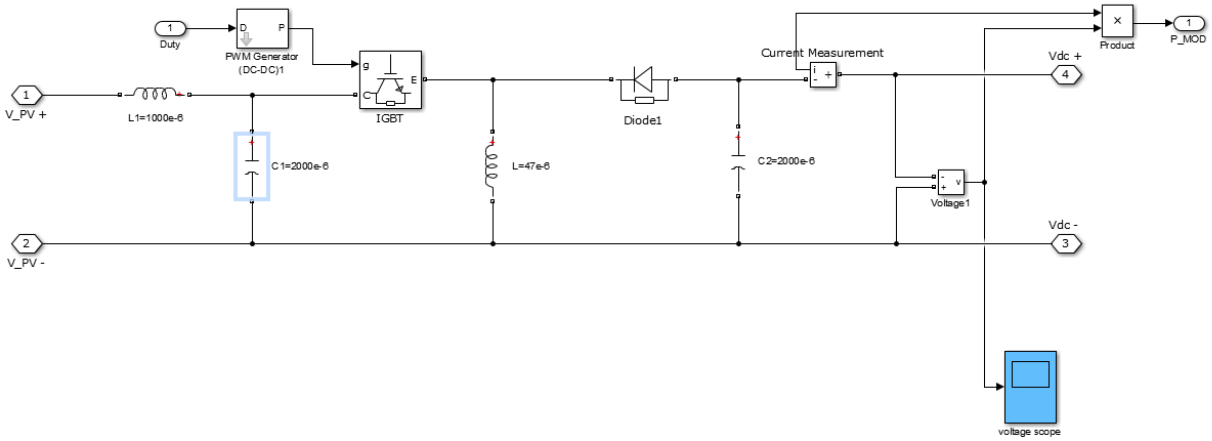

Figure 3.11: SIMULINK model for Buck-boost DC-DC converter.

4.2. P&O controller

We tested the P&O algorithm. With single PV module under uniform condition (G=1000 W/m²) as shown in figure 3.12.

The initializations used in the P&O algorithm are:

Table 3.3: Initial values for P&O algorithm.

Incrementation (deltaD)	V_{old}	P_{old}	$D_{initial}$
0.01	0V	0V	0.1

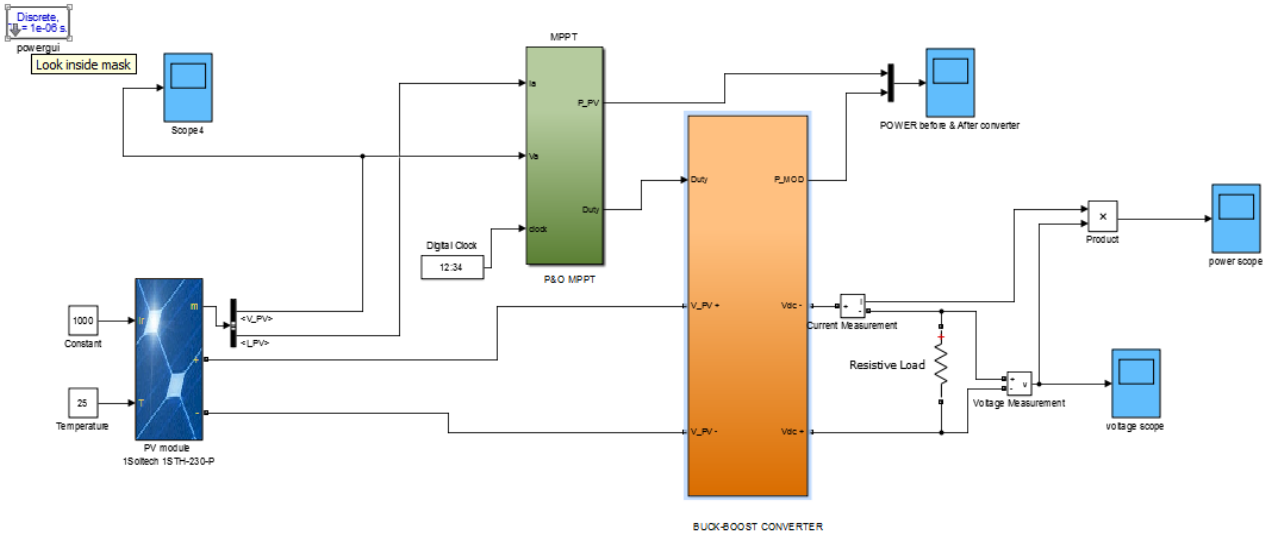

Figure 3.12: SIMULINK model for single PV-module under uniform condition using P&O controller.

The power curve of the simulation is shown below in figure 3.13.

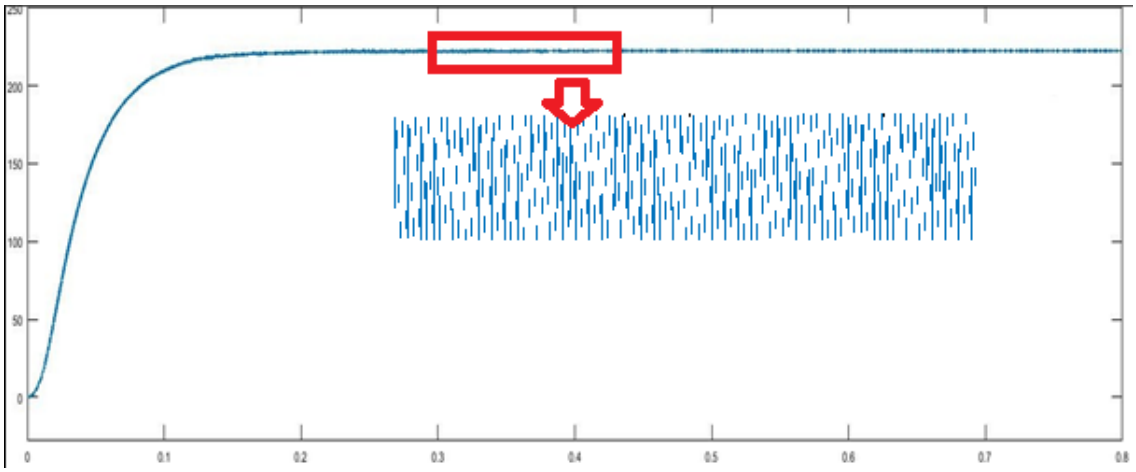

Figure 3.13: Power curve for single module under uniform condition using P&O controller.

To observe the behavior of the P&O algorithm with partial shading condition, we have connected four (4) PV modules in series, with DC-DC converter and the P&O controller. We used different irradiance values, where one module at full sun (1000 W/m²) and the others are 800 W/m^2, 500W/m^2 and 300 W/m^2.

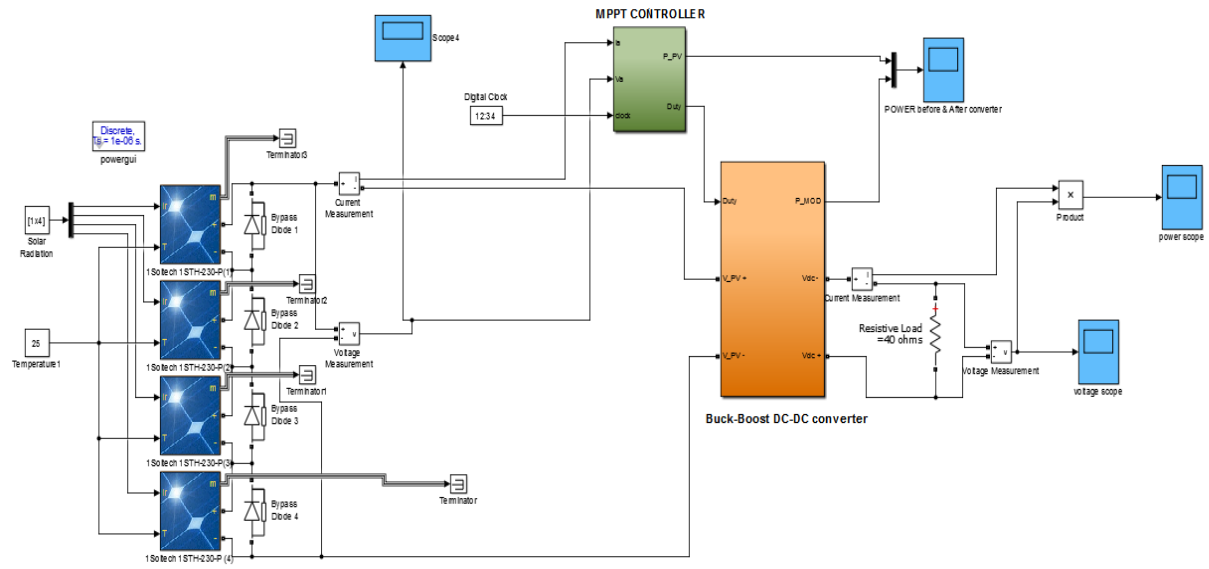

Figure 3.14: SIMULINK model for the system under PSC using P&O controller.

The resulting and PV curve of four (04) PV modules in series for PSC using P&O algorithm are shown in figure 3.15.

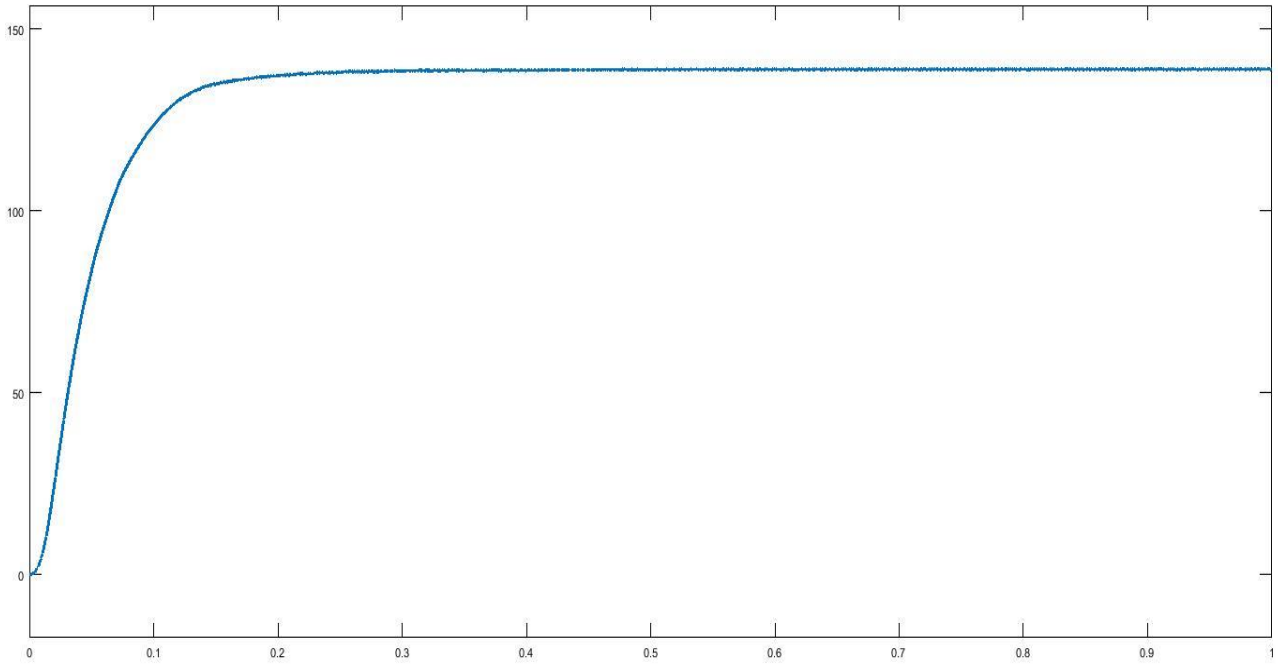

Figure 3.15: Power curve for 4 series connected modules under PSC using P&O controller.

We can see that the P&O controller is not useful in the partial shading conditions, because it can track only the first peak value which represent the local power point and cannot fix the power on the global power point.

4.3. PSO controller

4.3.1.PSO controller with single PV module in normal condition

We tested the PSO algorithm. With single PV module under uniform condition (G=1000 W/m², 25°C) as shown in figure 3.16.

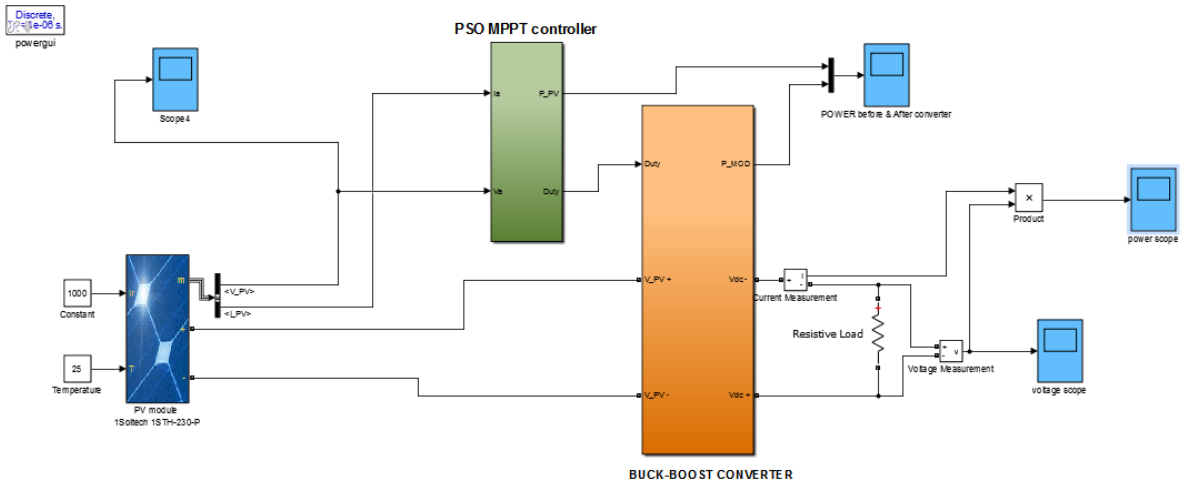

Figure 3.16: SIMULINK model for the system for a single PV module under uniform condition using PSO controller.

The initializations used in the PSO algorithm are:

Table 3.4: PSO based on MPPT algorithm equations constants.

ω(inertia weight)	C_1	C_2	R_1	R_2
0.4	1.2	1.6	random	random

Table 3.5: Initial values for PSO based on MPPT algorithm.

Number of iteration	12
Swarm size	4
Initial duty cycle (D)	[0.2 0.5 0.8]
Initial velocity	[0.001 0.001 0.001]
Personal best of D	[0 0 0]
Global best of D	0

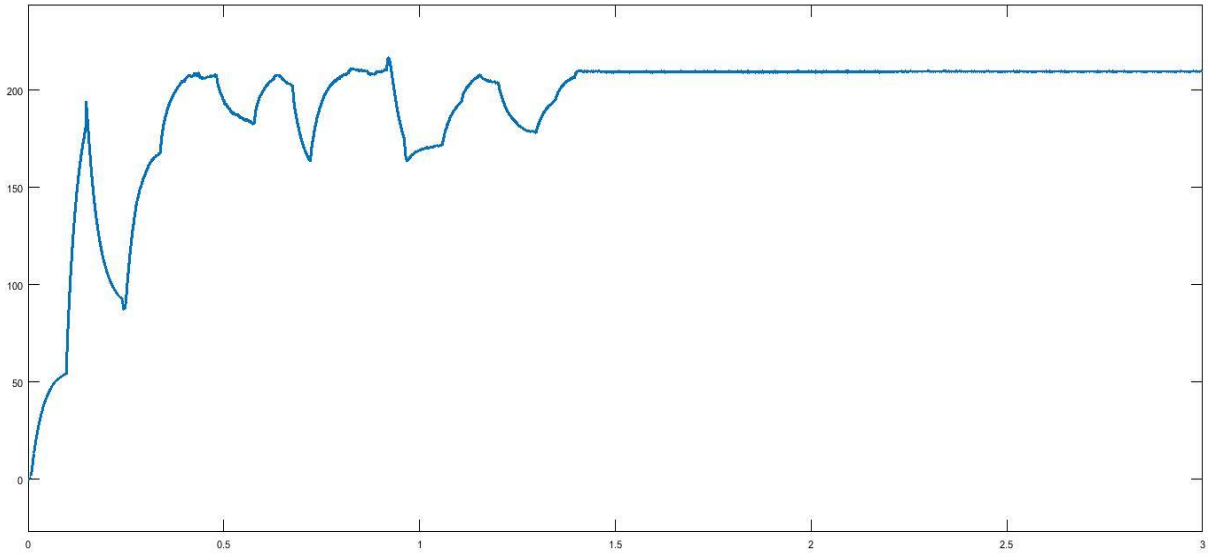

Figure 3.17: Power curve for single module under normal condition using PSO controller.

As we can see the PSO algorithm performs many oscillations when searching for the GMPP passing by LMPP until it will converge to the peak point which is the maximum power of our panel which is 228.735 W.

4-3-2 PSO controller for 4 series connected PV modules in PSC

To verify how the PSO algorithm can track global maximum power in partial shading condition. We have connected four (4) PV modules in series, with DC-DC buck-boost

converter and the PSO controller. We used different irradiance values, where one module at full sun (1000 W/m², 25°C) and the others are (800 W/m^2, 500W/m^2 and 300 W/m^2; 25°C) respectively.

The SIMULINK model is shown in the figure 3.18.

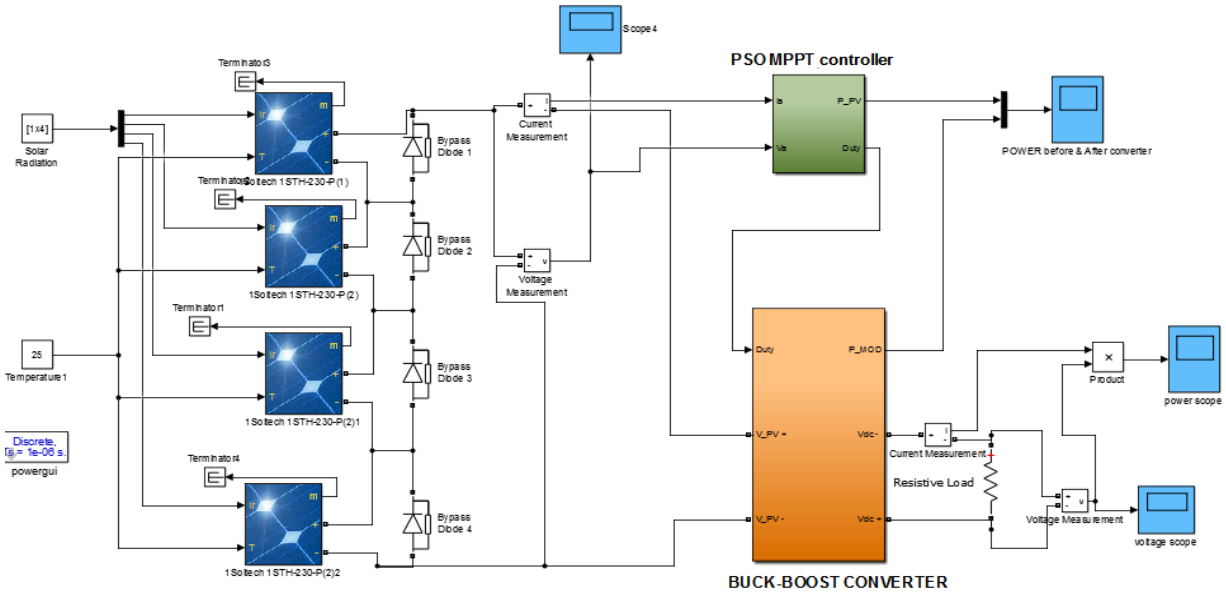

Figure 3.18: SIMULINK model for the system of 4 panels under PSC using PSO controller.

The corresponding I-V and P-V curves model for 4 series connected modules under PSC are shown in Figure 3.19.

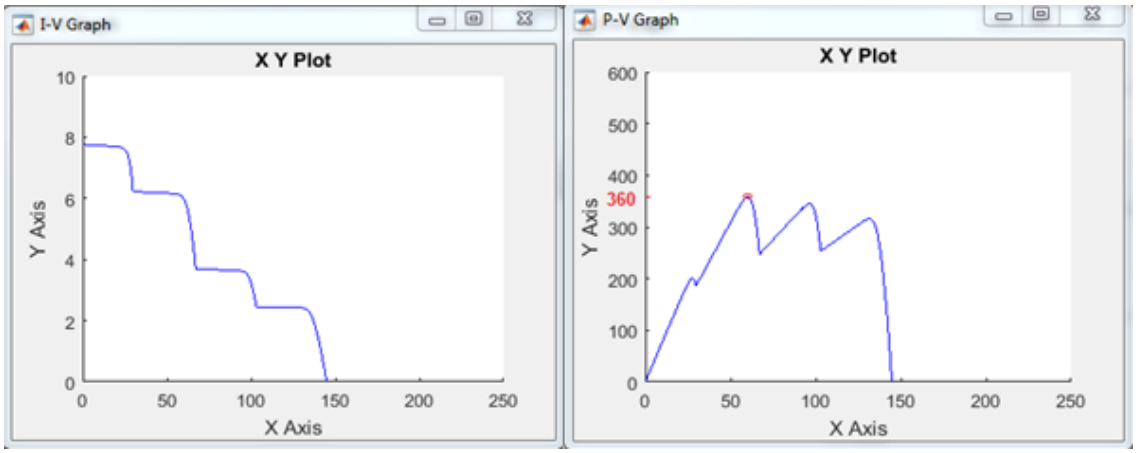

Figure 3.19: I-V and P-V curves model for 4 series connected modules under PSC using PSO controller.

The power curve after the simulation is show in figure 3.20.

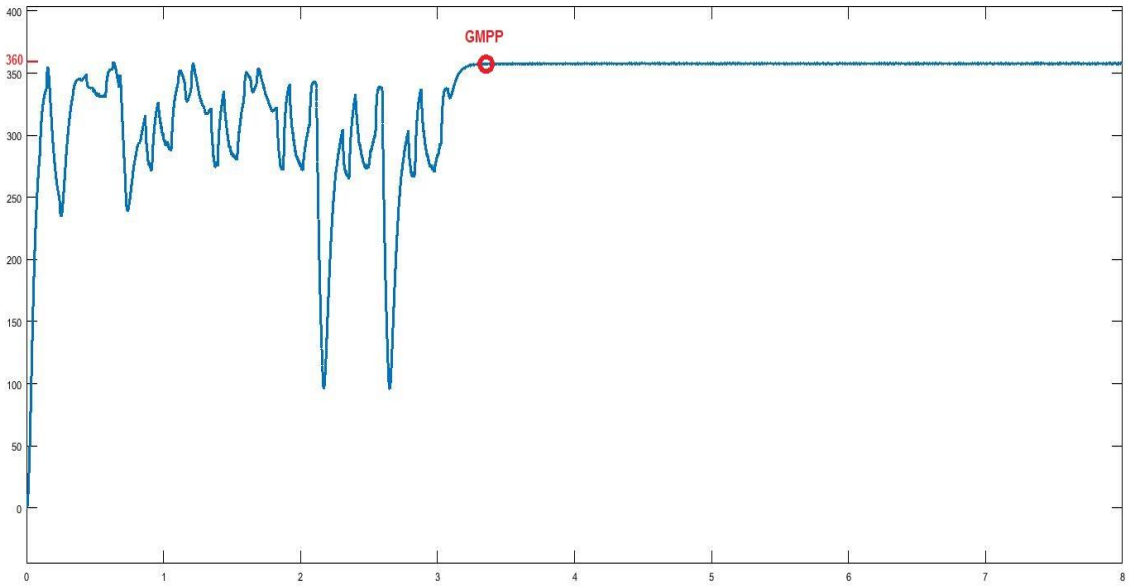

Figure 3.20: Power curve of four (4) PV-modules under PSC using PSO controller.

From the curve of the figure 3.20 we can see the oscillations performed by the PSO algorithm when searching for the GMPP, where it performs many tests for each iteration, until it reaches the value of 360W which represents the GMPP according to the curves in figure 3.19

To prove the efficiency of our algorithm we used to simulate it with different number of PV panels. Figures3.21and 3.22showthe Simulink model of PSO under PS conditions using 5 series PV panels with (1000 W/m^2,800 W/m^2, 500W/m^2, 300 W/m^2,200W/m^2) respectively at 25°Cand their I-V and P-V curves.

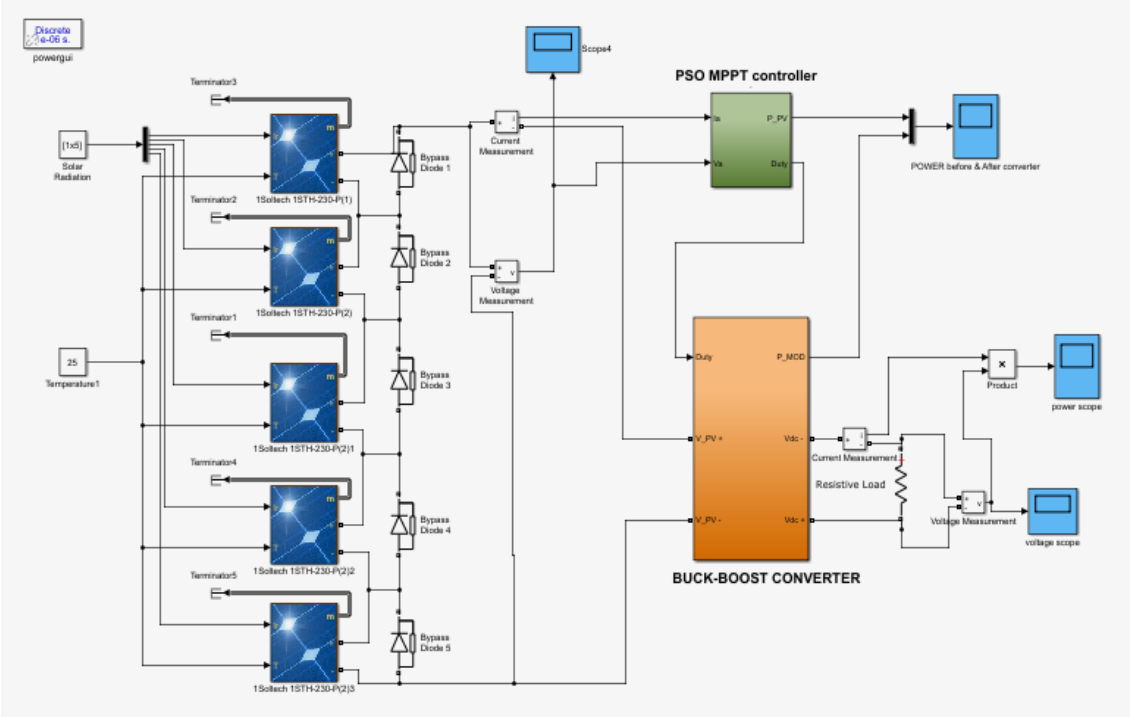

3.21: SIMULINK model for system with 5 panels under PSC using PSO controller.

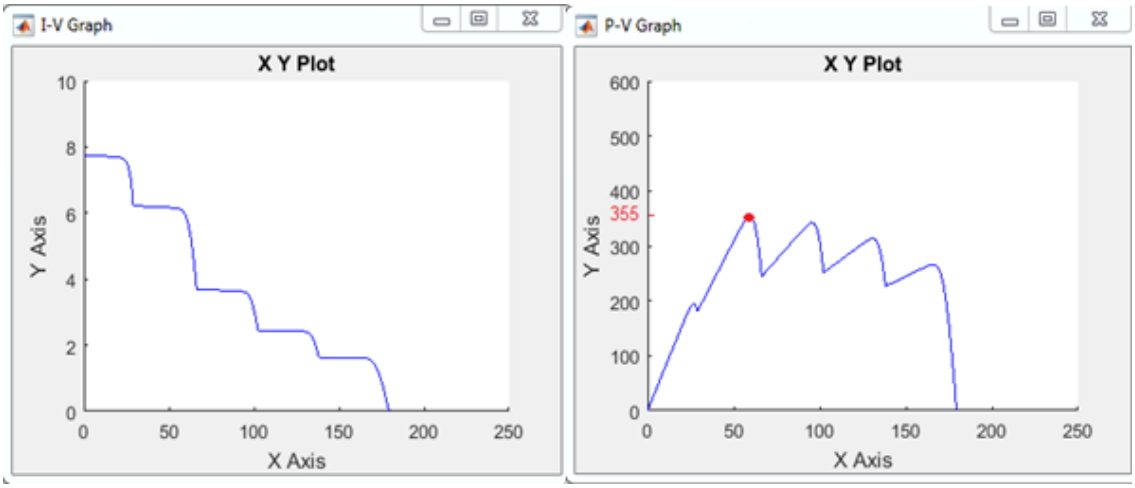

Figure 3.22: I-V and P-V curves model for 4 series connected modules under PSC using PSO controller.

The power curve after the simulation is show in figure 3.23.

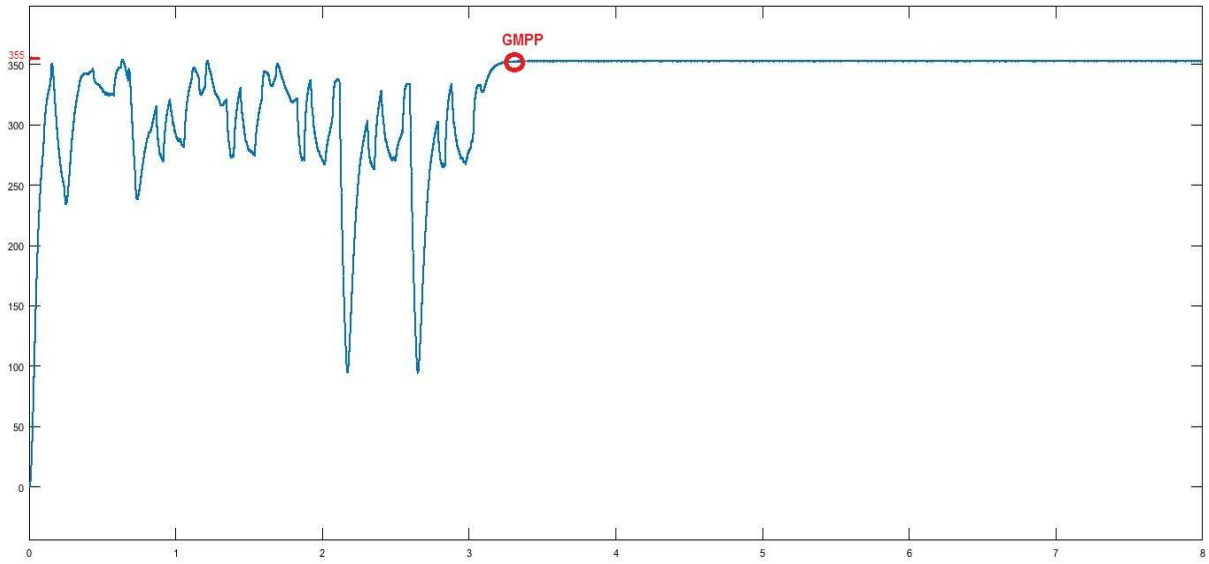

Figure 3.23: Power curve of five (5) PV-modules under PSC using PSO controller.

5. Discussion

- Figure 3.8shows that the absence of diode protection causes a decrease in current, due to the power dissipated in the shaded parts of the PV module.

- Due to non-uniform solar irradiance, the resulting P-V and I-V characteristic curves of the solar panel exhibits multi-peaks as shown in figures 3.10.

- From the results obtained in figure 3.13, we observe the effect of the applied algorithms on the maximum power point, once the maximum power is reached the system stabilized at this value. For the P&O, there will be an oscillation around that value due to the perturbation of the duty cycle as shown in figure 3.13. While for PSO, there is no oscillation, because, after several iterations the velocity goes to zero.

- Under partial shading, most conventional MPPTs cannot find the global maximum point. As we can see in figure 3.15 P&O is trapped at the first local maximum power causing significant power loss. This makes it totally incapable of handling partial shading conditions. Whereas, PSO algorithm shows a great ability to distinguish between local and global peaks as illustrated infigures3.20 and 3.23.

- The developed PSO algorithm was tested with many number of panels and it is found that it works well and tracks the GMPP regardless the PSC.

Chapter Four:

Implementation and Results

1. Introduction

After the completion of the described system's simulation we will move to implementation part. In this part we will implement the P&O algorithm with simple panel under normal condition. This implementation must be designed according to well defined standards and specifications. This work is divided into two parts: control and power circuits. Each part of the system is implemented and tested. In this chapter the design and implementation of the MPPT controller is covered where digital control is chosen. Each implemented circuit is explained in details, and the obtained results are discussed by the end.

The photovoltaic panel used is the one available in laboratory (SUNTECH STP050D-12MEA) made of 36 series connected poly crystalline cells, (Appendix C). Its technical characteristics are given in table 4.1.

Table 4.1: SUNTECH STP050D-12MEA Characteristics under STC.

P_{max}	$50\ W$
V_{oc}	$21.8\ V$
V_{mp}	$17.4\ V$
I_{sc}	$3.13\ A$
I_{mp}	$2.93A$

The proposed MPPT scheme is shown in Fig 4.1. The controller consists of two blocks, power stage and control unit.

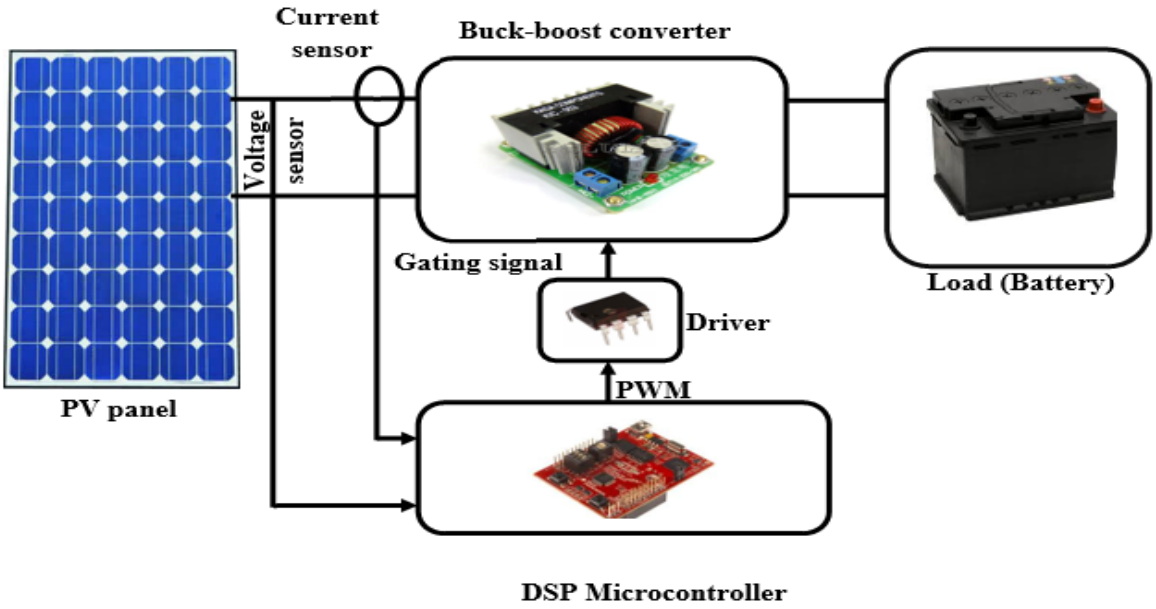

Figure4.1. PV panel with MPPT controller.

The methodology followed in implementing the proposed MPPT controller is:

- Designing and sizing the power stage (inductor, capacitor, switching elements).
- Designing the control unit.
- Design of the measurement unit.
- Components choice.
- Implementation of the prototype.

2. Switching element

A large variety of power switches with different characteristics and control requirements are available nowadays namely, BJTs, IGBTs, MOSFETs, GTOs…ext. In terms of control, voltage controlled devices are preferred owing the ease of generating their gating (control) signal. Due to that fact, IGBTs and MOSFETs are selected.

The choice between MOSFETs and IGBTs is based on the power and voltage ratings, in addition to their maximum switching frequency. According to, IGBTs are best for low-frequency, high-voltage and high-power applications, whereas, MOSFETs for high-frequency, low-voltage and high-power applications [13].

Fig.4.2.1 shows the different operating regions of IGBT and MOSFET switches.

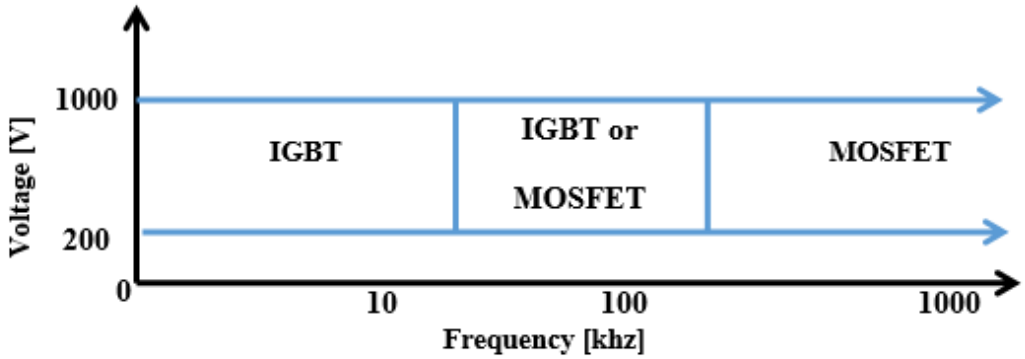

Figure 4.2: Appropriate operating regions of MOSFETs & IGBTs.

In this MPPT design, the maximum power and voltage are $P_{max} = 50W$,$V_{max} = V_{oc} = 21.8V$, the switching frequency$f_s = 10khz$, the decision to choose the IGBT is obvious.

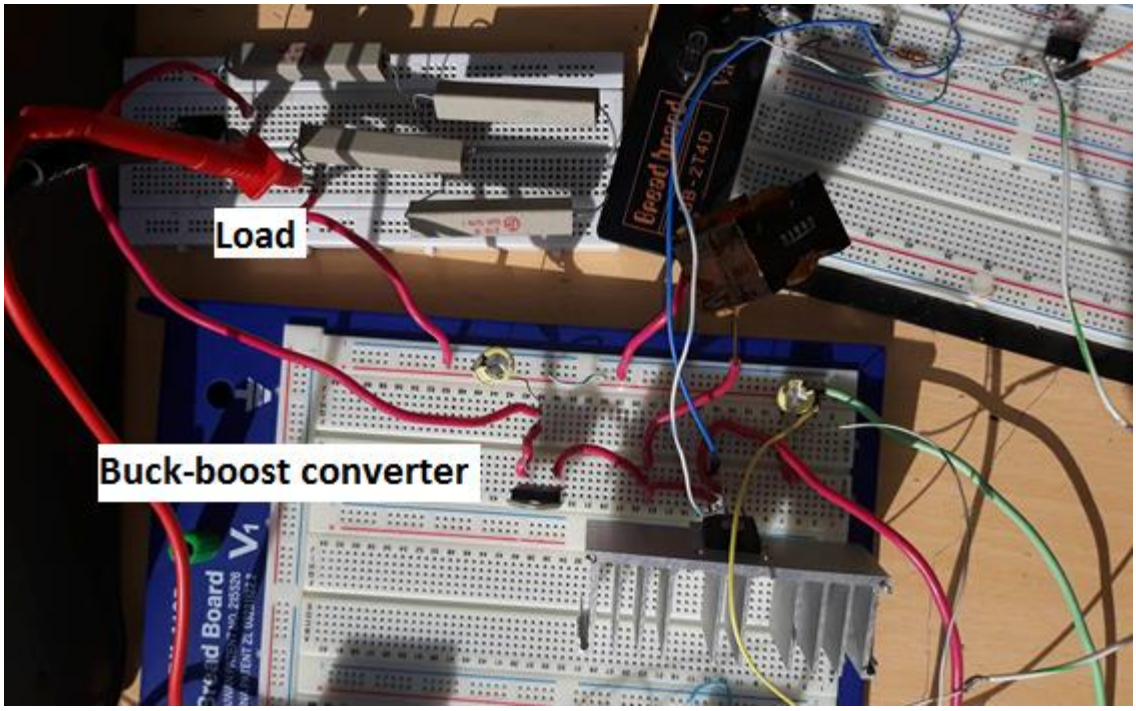

Figure 4.3: DC-DC buck-boost converter implementation connected to the load.

3. Control unit

The control unit is the area where the algorithm performs calculations and decisions. Many controllers are available in commercial scale like AVR, PIC, DSP…. etc. In this design DSP MicrocontrollerLAUNCHXL-F28027F from TEXAS INSTRUMENTS is chosen. This microcontroller contains ADCs and PWM pins. The needed Microcontroller

must fulfill the following requirements: Two (2) Analog to Digital channels (ADC), a PWM output channel and a sufficient memory size, (Appendix B).

4. Drive circuit of the transistor gate

The output pulse signals of the DSP controller have a voltage level of 3.3 V with low energy, however, the required gate voltage signals to drive the IGBT is at least voltage 15 V with high energy. As a result, a driver circuit, which has the function as a power amplifier and isolator is needed to amplify low-power digital pulse signals to high-power electrical pulse signals to drive the IGBT as well as isolate and protect the microcontroller. The gate driver used here is the HCNW3120 from AVAGO Technologies with 2.5 Amp Output Current. The schematic of the gate driver circuit is shown in Figure 4.4.

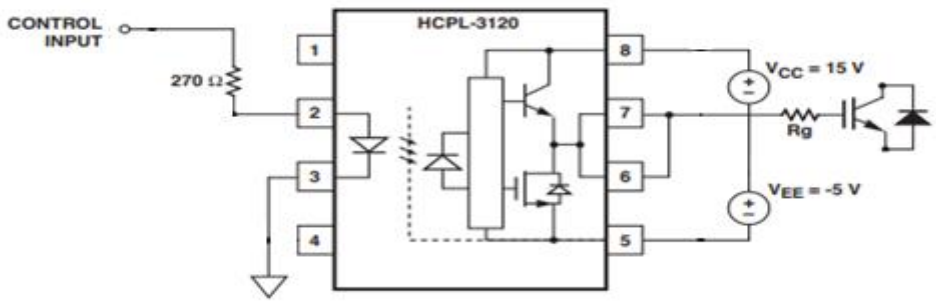

Figure 4.4: Schematic of the IGBT gate driver circuit.

4.1. Power supply of the drive circuit of the IGBT

To ensure the +15V and -5V DC we implemented the circuit shown Figure 4.5. It acts as a power supply with a common ground. It is made of: a step down center-tape transformer that drops the 230 V AC to 15 V AC, a bridge rectifier, for signal rectification, 1000µF in parallel with resistor and Zener diode which generates the desired +15V DC and -5V DC. This power supply is used to supply the drive circuit of the IGBT.

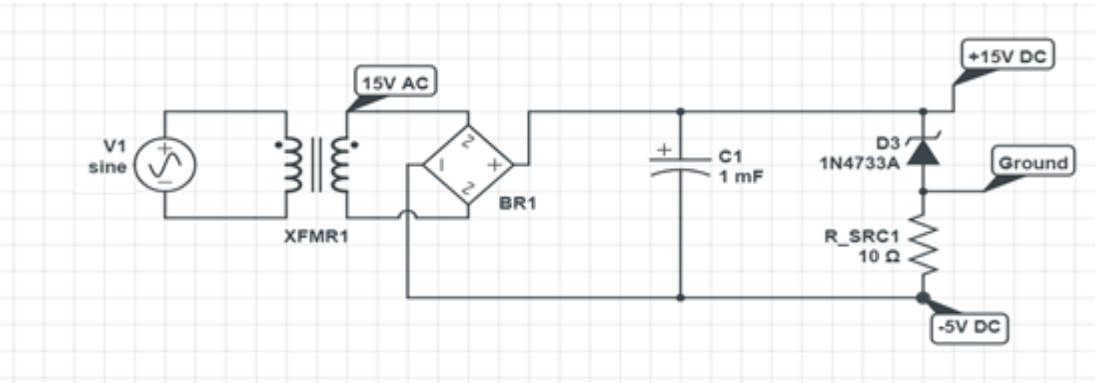

Figure 4.5: Schematic of power supply of drive circuit of IGBT.

5. Voltage and current measurements

In order to calculate P_{pv}, the controller needs to measure $I_{pv}$and V_{pv} using voltage and current measurement instruments.

5. 1. Voltage measurement

The Microcontroller has the ability to measure voltage within the range of [0-3.3V] using its ADC. However,V_{pv} exceeds the allowed interval.

Voltage transducer LV25-P from LEM is selected to measure the DC voltage of the PV-panel. The nominal RMS current of the primary side is 10 mA and the nominal RMS current of the secondary side is 25mA. By selecting proper external resistance in the primary circuit, the voltage transducer can measure voltages with amplitude in the range of 10 V to 500 V. In order to measure the voltage, a current proportional to the voltage must pass the primary circuit. By setting value of the external resistors in the secondary circuit the ratio between the output and the input of the voltage transducer can be determined. As the output signal of the sensing circuit is the input signal of the DSP controller, the voltage range of the signal should be limited within 0V to 3.3 V, otherwise it will damage the DSP controller. Besides, there is no DC offset of the output of the voltage transducer, which means when the input voltage is 0V the output voltage is 0V. The schematic of the DC voltage sensing circuit shown in Figure4.6.

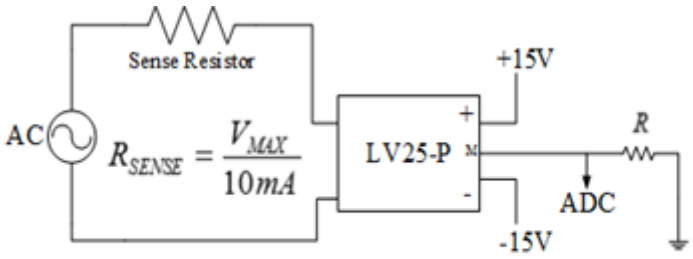

Figure 4.6: Schematic of the DC voltage sensing circuit.

We have chosen a resistor of 3KΩ in the primary to reduce the current coming from the PV-panel to not exceed 10 mA. And a resistor of 100 Ω to ensure that the input voltage of the DSP doesn't exceed 3.3V.

5.2. Current measurement

The Microcontroller cannot measure the current. I_{pv}. It must be converted to a voltage quantity which is the image of the actual current. Several methods can be used to do this conversion.

5.2.1: Current Sensor

LA 25-P from LEM Hall Effect current transducer is used to measure I_{pv}. Figure.4.7 below shows its typical connection.

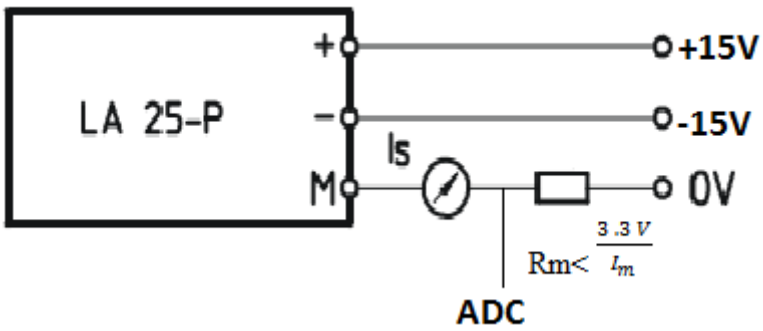

Figure 4.7: LA 25-P connection.

This sensor has an excellent accuracy, high immunity to external interference with a very good linearity. It also provides galvanic isolation between primary and the secondary circuits.

To get better resolution, the sensor is supplied with $V = \pm 15V$, the measurement resistance is set to $R_M = 470\Omega$.

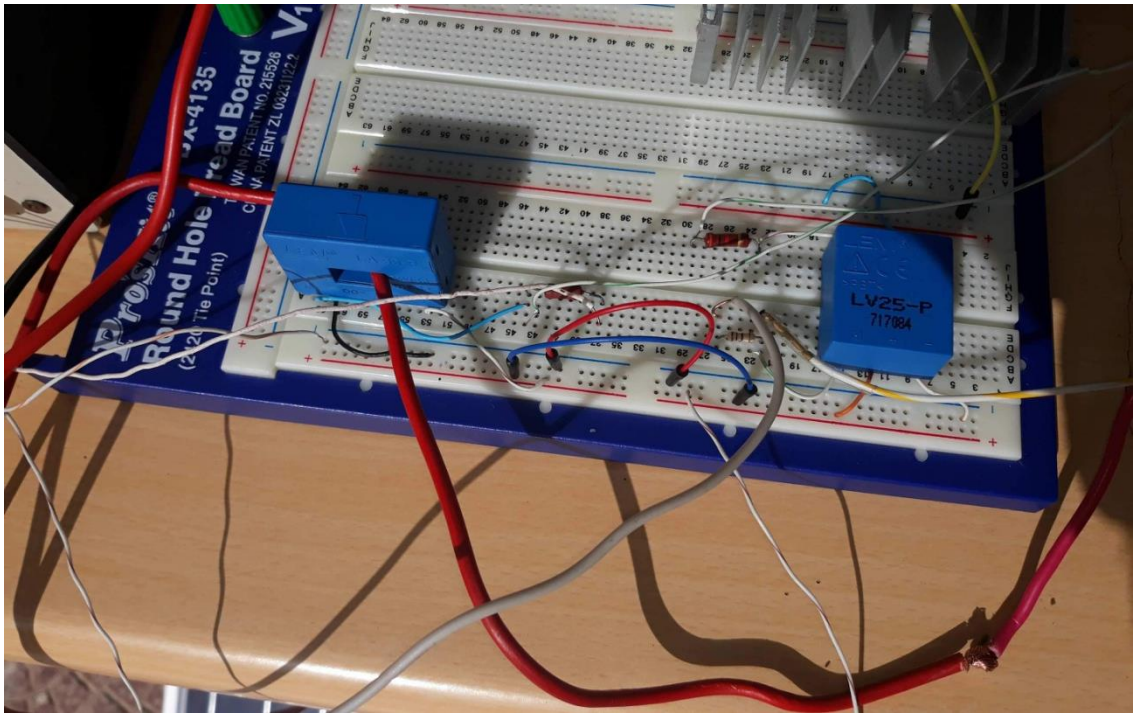

Figure 4.8: Current and voltage sensors prototype set up.

6. Prototype presentation

The power and control circuits are built. The control stage is built in SIMULINK and loaded into the DSP to generate PWM with frequency of 10 KHz. The power converter, gate drive circuit, voltage and current sensors circuit are built on a prototyping board.

The required power inductor value ($L = 47\mu H$) is not available in commercial scale; we have used a power inductor of (L= 1.43 mH) because it is the only one available in the laboratory. Except the inductor, all other components are available and widely used.

Due to the unavailability of identical panels in the laboratory we could not implement the prototype for PSO algorithm, only P&O was implemented. The P&O MPPT algorithm is written using MATLAB code then uploaded in the DSP Microcontroller via SIMULINK. The DSP is set to pulsate at 10 KHz Pins (ADCIN A0) and ($ADCINA1$) are initialized to operate as analog to digital converters (ADC_s). Voltage measurement (V_{pv}) is done through ($ADCINA0$) which is connected to the voltage measurement, else, ($ADCINA1$)receives the current measurement from the Hall Effect sensor. Pin

(EPWM1A) generates the PWM signal. This PWM signal turns the IGBT ON and OFF. The switching action of the power IGBT allows the variation of V_{pv}.

The buck-boost converter was tested with a constant duty cycle PWM and DC-supply.

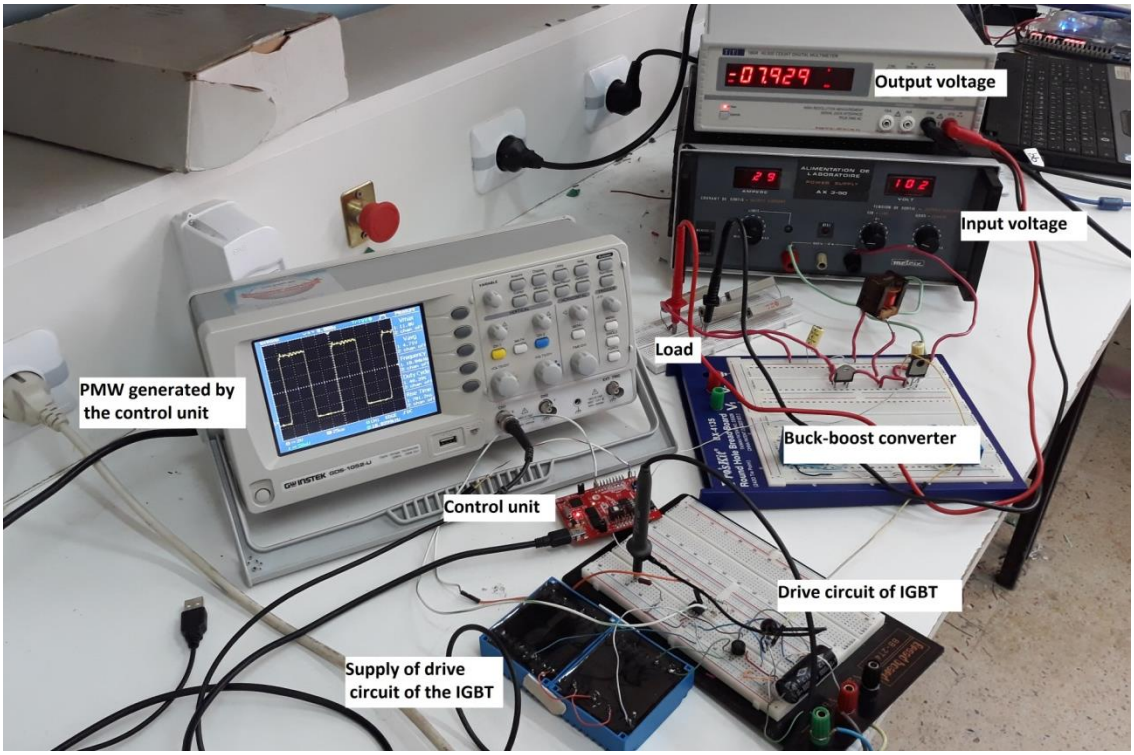

Figure 4.9: Test circuit of the DC-DC buck-boost converter.

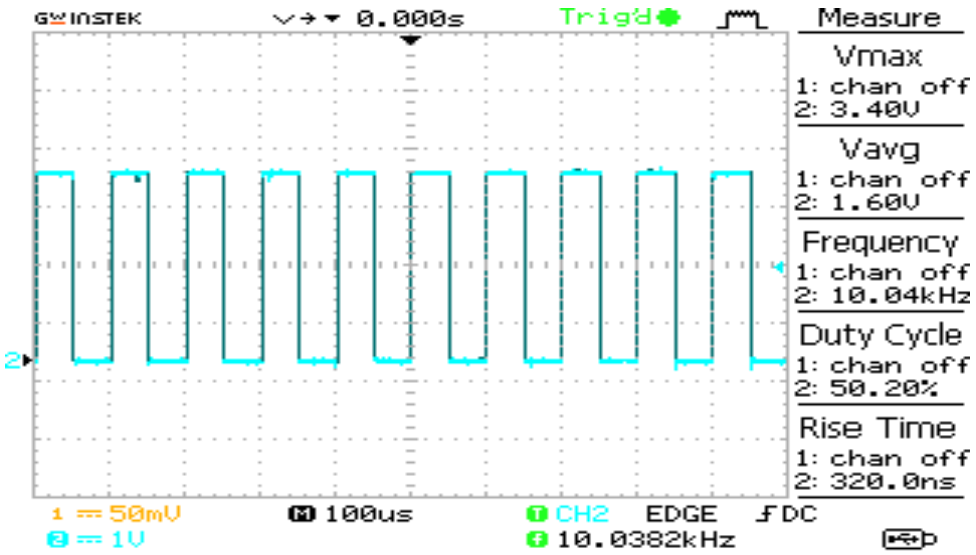

Figure4.10: PWM signal generated by the DSP microcontroller (by assuming V_{pv} and I_{pv} as constant).

Now we will move to the real implementation using current and voltage sensors with ADCs and a real PV-panel.

Since the unavailability of an instrument to measure the irradiance and temperature, so we don't know the maximum power that this PV panel can generate under the climatic condition when the experiment occurred. Then we have to test that by implementing a circuit composed of PV-panel and a variable power resistor is series.

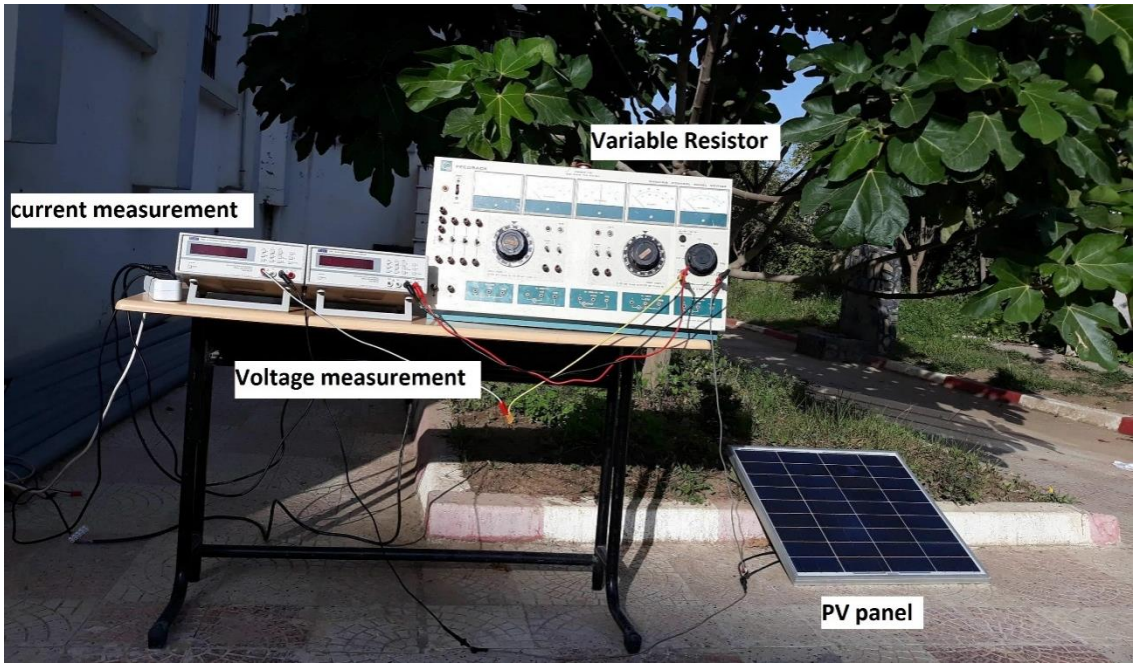

Figure 4.11: Implemented circuit used to determine PV-curve of the panel.

We have to change the value of the resistor from its minimum (short circuit test) to its maximum (open circuit test), and each time we measure the voltage and current and calculate the power. The collected data are shown in table 4.1.

Table 4.1: Measured power and voltage of the PV-panel.

V_{pv}	3.4	11.42	13	15	17.57	18.1	18.22	18.53	18.73	18.8	18.92	18.98	18.42
P_{pv}	8.84	26.72	32.5	37	39.7	37.1	27	14.82	14.54	12	10.97	9.11	8.9
V_{pv}	19	19.26	19.2	19.14	19.17	19.3	19.32	19.33	19.34	19.35	19.4	19.45	19.5
P_{pv}	8.55	8.28	7.48	6.69	6.13	4.83	3.86	3.09	2.51	1.5	1.37	1.2	1

Using Matlab, we have summarized our table in the curve shown in figure 4.12:

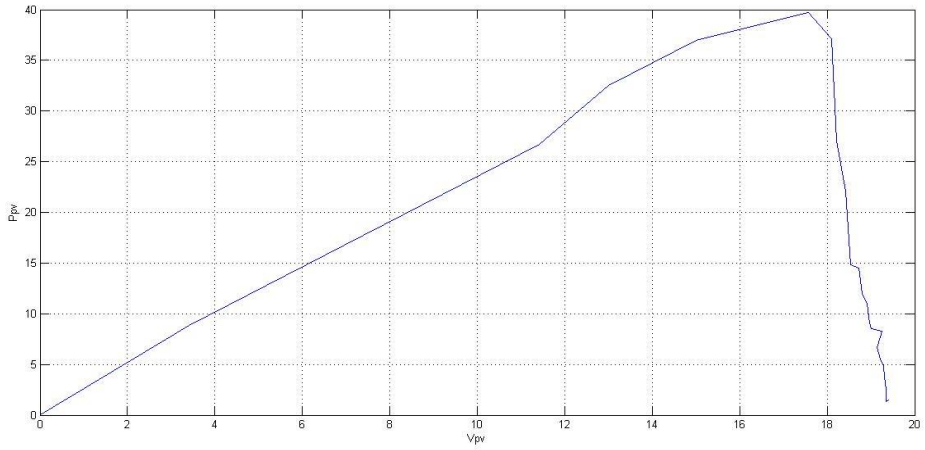

Figure 4.12: P-V curve under climatic condition of the experiment.

Then, the whole hardware set up configuration was implemented using PV-Panel and current and voltage sensors.

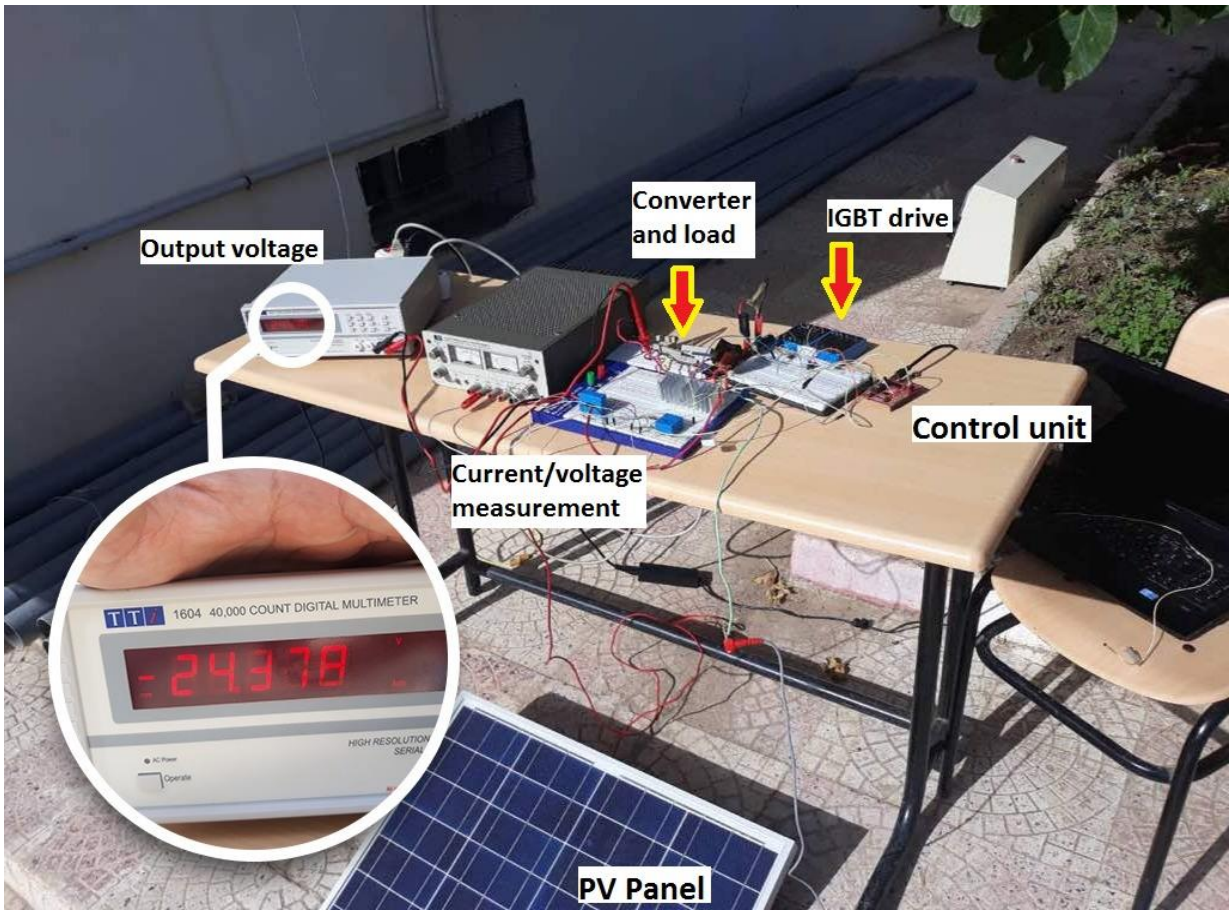

Figure 4.13: Implementation of the whole system.

7. Conclusion

In this chapter the different steps and methodology for the design and the implementation of MPPT controller is covered. As a 1st step, the power stage components are selected based on theoretical calculations and required specifications.

The control unit is designed based on DSP microcontroller. Secondly the implementation of buck-boost converter is tested separately as shown previously. Finally, the whole system was implemented using a PV-panel and the results are satisfying theoretical part.

Although the difficult availability of components and electrical devices, the prototype is totally completed with the accessible material and resources.

General Conclusion

General conclusion

In order to design a perfect stand-alone PV system, it is necessary to maintain the PV power at its maximum. The presented work dealt with the analysis, design, simulation and implementation of a Stand-alone Photovoltaic System, using DSP C2000.

The goal of our work was to extract the maximum power from the panel using different algorithms such as the conventional one P&O and the new one PSO then comparing the results to show the efficiency of the PSO algorithm on extracting the GMPP even if there are changes in the irradiance. This work is tested using MATLAB/Simulink Software and then implemented using PV-Panel and DSP microcontroller.

The proposed technique was tested under STC, after that changing conditions with different step variations on irradiance and finally under partial shading. When MPPT is used there is no need to input the duty cycle, the algorithm iterates and decides the duty cycle by itself. But if MPPT had not been used, then the user would have had to input the duty cycle to the system. Where there is change in the solar irradiation the maximum power point changes and thus the required duty cycle for the operation of the model also changes. But if constant duty cycle is used then maximum power point cannot be tracked and thus the system is less efficient. It must be mentioned that, the panel used in the simulation was a 228.7W; however, in the implementation, only one module of 50W was available.

The objectives of the project were achieved as well as the comprehensive understanding of PV systems. It is also shown that the PSO algorithm has many advantages such as Fast tracking speed and It exhibits no oscillations around the MPP, also It can provide an accurate and reliable tracking performance of the MPP when changes on irradiance or temperature occur. Finally, the proposed algorithm shows a great ability to distinguish between local and global peaks which mean tracking the true MPP under partial shading.

REFERENCES

References

[1] J. Surya Kumari and Ch. Sai Babu, "Mathematical Modeling and Simulation of Photovoltaic Cell using Matlab-Simulink Environment" ,(Vol. 2, No. 1, February 2012, pp. 26~34).

[2] Syahrul Ashikin Azmi PPKSE, "Photovoltaic Material And Electrical Characteristic".

[3] M.G.Villalva, J.R.Gazoli and E. Ruppert F. "Comprehensive Approach to Modeling and Simulation of Photovoltaic Arrays". IEEE Transactions on power electronics.(Vol.24, No. 5, 2009. pp 1198 – 1208).

[4] Z. Sen. "Solar energy in progress and future research trends." Progress in Energy and Combustion Science". (2015, 30, pp. 367-416.)

[5] Marcelo. G and al, "Comprehensive Approach to Modeling and Simulation of Photovoltaic Arrays," *IEEE Transactions on Power Electronics* (May 2009, Vol. 24, NO. 5,.)

[6] Sergio Daher, Jurgen Schmid and Fernando L.M Antunes, "Multilevel Inverter Topologies for Stand-Alone PV Systems*" .(* July 2008. IEEE Transactions on Industrial Electronics.Vol.55, No.7)

[7] Nicola, F.; Giovanni, P.; Giovanni, S.; Massimo, V. "Optimization of perturb and observe maximum power point tracking method". IEEE Trans. Power Electron.(**2005**, 20, 963–973.)

[8] Mamarelis, E.; Petrone, G.; Spagnuolo, G. "A two-steps algorithm improving the P & O steady state MPPT efficiency". (Appl. Energy **2014**, 113, 414–421.)

[9] Ramdan B. A. Koad, Ahmed. F. Zobaa, "Comparison between the Conventional Methods and PSO Based MPPT Algorithm for Photovoltaic Systems".

[10] T. Esram and P. L. Chapman, "Comparison of Photovoltaic Array Maximum Power Point Tracking Techniques," Energy Conversion, IEEE Transactions on, (vol. 22, pp. 439-449, 2007.)

[11] Ramdan B. A. Koad , Ahmed F. Zobaa, Senior Member, IEEE and Adel El-Shahat, "A Novel MPPT Algorithm Based on Particle Swarm Optimisation for Photovoltaic Systems".

[12] K. Ishaque and Z. Salam, "A deterministic particle swarm optimization maximum power point tracker for photovoltaic system under partial shading condition," *IEEE Trans. Ind. Electron.(* Aug. 2013, vol. 60, no. 8, pp. 3195–3206).

[13] A. Durgadevi, S. Arulselvi and S. Natarajan, "Study and implementation of maximum power point tracking (MPPT) algorithm for photovoltaic systems," in Electrical Energy Systems (ICEES). (2011 1st International Conference on. 2011, pp. 240-245).

APPENDICES

Appendix A: Buck-Boost converter parameters calculation

1. Selection of the buck-boost converter parameters:

The necessary data needed to estimate the buck-boost converter parameter are shown in the table A.1.

Table A.1: Needed data in computation of buck-boost converter

Description	**Parameter**	**Unit**
Input voltage range	$V_{I(min)}$ to V_{IM}	V
Output voltage	V_O	V
Maximum average output current	I_{OM}	A
Allowed inductor current ripple	$I_{(L1)(PP)}$	mA
Switching frequency of the internal switch S1	$f_{(SW)}$	kHz

the DC conversion ratio V_O / V_I:

$$\frac{V_0}{V_i} = \frac{-D}{1-D} \quad \text{A.1}$$

3.1. Selection of the Inductor:

The required inductance:

$$L1 = \frac{V_i\, D}{I_{(L1)(pp)} f_{(sw)}} \quad \text{A.2}$$

3.2. Select the Rectifier Diode:

Generally, it is recommended to use Schottky diodes for inductive low- to middle-power DC/DC converters. This is due to the low forward voltage drop which leads to higher efficiency.

3.3. Selection of the capacitors:

The minimum effective value for this capacitor $C_{1(min)}$can be estimated with:

$$C_{1(min)} = \frac{I_{(L1)(AVG)} \times D}{f_{(sw)} \times [V_{i(pp)} - (I_{(L1)(pp)} \times ESR_{CI})]} \dots\dots\dots\dots\dots\dots\dots\dots\dots\dots\dots\dots\dots\dots A.3$$

The minimum required capacitance $C_{O(min)}$ at an output voltage ripple requirement of $V_{O(PP)}$, given by:

$$C_{o(min)} = \frac{I_o \times D}{f_{(sw)} \times \left[V_{o(pp)} - \left(\frac{I_o}{1-D} + \frac{I_{(L1)(pp)}}{2}\right) \times ESR_{co}\right]} \dots\dots\dots\dots\dots\dots\dots\dots\dots\dots A.4$$

Appendix B: DSP TMS320f28027f

S

.

Mux Value						Mux Value			
3	2	1	0	J1 Pin	J5 Pin	0	1	2	3
			+3.3V	1	1	+5V			
			ADCINA6	2	2	GND			
TZ2	SDAA	SCIRXDA	GPIO28	3	3	ADCINA7			
TZ3	SCLA	SCITXDA	GPIO29	4	4	ADCINA3			
Rsvd	Rsvd	COMP2OUT	GPIO34	5	5	ADCINA1			
			ADCINA4	6	6	ADCINA0			
	SCITXDA	SPICLK	GPIO18	7	7	ADCINB1			
			ADCINA2	8	8	ADCINB3			
			ADCINB2	9	9	ADCINB7			
			ADCINB4	10	10	NC			
3	2	1	0	J6 Pin	J2 Pin	0	1	2	3
Rsvd	Rsvd	EPWM1A	GPIO0	1	1	GND			
COMP1OUT	Rsvd	EPWM1B	GPIO1	2	2	GPIO19	SPISTEA	SCIRXDA	ECAP1
Rsvd	Rsvd	EPWM2A	GPIO2	3	3	GPIO12	TZ1	SCITXDA	Rsvd
COMP2OUT	Rsvd	EPWM2B	GPIO3	4	4	NC			
Rsvd	Rsvd	EPWM3A	GPIO4	5	5	RESET#			
ECAP1	Rsvd	EPWM3B	GPIO5	6	6	GPIO16/32	SPISIMOA/ SDAA	Rsvd/ EPWMSYNCI	TZ2/ ADCSOCA
TZ2/ ADCSOCA	Rsvd/ EPWMSYNCI	SPISIMOA/ SDAA	GPIO16/32	7	7	GPIO17/33	SPISOMIA/ SCLA	Rsvd/ EPWMSYNCO	TZ3/ ADCSOCB
TZ3/ ADCSOCB	Rsvd/ EPWMSYNCO	SPISOMIA/ SCLA	GPIO17/33	8	8	GPIO6	EPWM4A	EPWMSYNCI	EPWMSYNCO
			NC	9	9	GPIO7	EPWM4B	SCIRXDA	Rsvd
			NC	10	10	ADCINB6			

Table B.1: Pins' location on the DSP TMS320f28027f

Appendix C: Datasheet of PV-panels

PV Module 1STH-230-P Details

Return to product list...

Manufacturer: 1Soltech
Model Number: 1STH-230-P
Production Status: unknown
CSI Approved: Yes
CSI Model Number: 1STH-230-P
Description: 230W Polycrystalline Module

Electrical

Power at STC (W)	230
Power at PTC (W)	203.1
Bifacial	No
Bifaciality (%)	-
Lower Power Tolerance (%)	-
Upper Power Tolerance (%)	-
Power Density at STC (W / m2)	146.497
Power Density at PTC (W / m2)	129.363
Module Efficiency (%)	-
Cell Efficiency (%)	-
Vmp: Voltage at Max Power (V)	29.9
Imp: Current at Max Power (A)	7.65
Voc: Open Circuit Voltage (V)	37.1
Isc: Short Circuit Current (A)	8.18
Max System Voltage (V)	-
Series Fuse Rating (A)	-
Bypass Diode	-
Nominal Operating Cell Temp (°C)	47.4
Open Circuit Voltage Temp Coefficient (% / °C)	-0.361
Short Circuit Current Temp Coefficient (% / °C)	0.102
Max Power Temp Coefficient (% / °C)	-0.495

Figure C.1. Datasheet of 1-STH-230P used in simulation

SPECIFICATION CATEGORIES		Db Mono	Kb Poly	Cb Mono	Lb Poly	Rb Poly	Rb Poly	Md Poly	Md Poly	Sb Poly
		STP005B -12/DEA	STP010D -12/KEA	STP020B -12/CEA	STP030D -12/LEA	STP040D -12/REA	STP045D -12/REA	STP050D -12/MEA	STP055D -12/MEA	STP060D -12/SEA
ELECTRICAL CHARACTERISTICS	Open-Circuit Voltage (Voc)	21.6 V	21.6 V	21.7 V	21.6 V	21.8 V	22.0 V	21.8 V	22.2 V	21.6 V
	Optimum Operating Voltage (Vmp)	17.4 V	17.4 V	17.6 V	17.2 V	17.4 V	17.6 V	17.4 V	17.5 V	17.4 V
	Short-Circuit Current (Isc)	0.32 A	0.65 A	1.26 A	1.94 A	2.58 A	2.79 A	3.13 A	3.34 A	3.90 A
	Optimum Operating Current (Imp)	0.29 A	0.57 A	1.14 A	1.74 A	2.30 A	2.58 A	2.93 A	3.14 A	3.45 A
	Maximum Power at STC (Pmax)	5 Wp	10 Wp	20 Wp	30 Wp	40 Wp	45 Wp	50 Wp	55 Wp	60 Wp
	Operating Temperature	-40°C to +85°C	-40°C to +85°C	-40°C to +85°C	-40°C to +85°C	-40°C to +85°C	-40°C to +85°C	-40°C to +85°C	-40°C to +85°C	-40°C to +85°C
	Maximum System Voltage	715 V DC	715 V DC	715 V DC	715 V DC	715 V DC	715 V DC	715 V DC	715 V DC	715 V DC
	Maximum Series Fuse Rating	5 A	5 A	5 A	5 A	10 A	10 A	10 A	10 A	15 A
	Power Tolerance	±10 %	±10 %	±10 %	±10 %	±5 %	±5 %	±5 %	±5 %	±5 %
MECHANICAL CHARACTERISTICS	Solar Cell	Mono-crystalline solar cell	Poly-crystalline solar cell	Mono-crystalline solar cell	Poly-crystalline solar cell	Poly-crystalline solar cell	Poly-crystalline solar cell	Poly-crystalline solar cell	Poly-crystalline solar cell	Poly-crystalline solar cell
	No. of Cells	36 (4×9)	36 (6×6)	36 (2×18)	36 (4×9)	36 (4×9)	36 (4×9)	36 (4×9)	36 (4×9)	36 (4×9)
	Dimensions	216 × 306 × 18 mm	310 × 368 × 18 mm	656 × 306 × 18 mm	426 × 680 × 18 mm	537 × 665 × 30 mm	537 × 665 × 30 mm	631 × 665 × 30 mm	631 × 665 × 30 mm	771 × 665 × 30 mm
	Weight	0.8 kgs	1.5 kgs	2.5 kgs	3.2 kgs	4.5 kgs	4.5 kgs	6.4 kgs	6.4 kgs	6.2 kgs
	Junction Box	IP65 rated	IP65 rated	IP65 rated	IP65 rated	IP65 rated	IP65 rated	IP65 rated	IP65 rated	IP65 rated
	Output Cables	(Optional cable available)	(Optional cable available)	(Optional cable available)	(Optional cable available)	(Optional cable available)	(Optional cable available)	(Optional cable available)	(Optional cable available)	H+S (12 AWG) Lengths: 750mm(-) and 750mm(+) Connection: MC Plug Type IV
TEMP. CHARACTERISTICS	Nominal Operating Cell Temperature (NOCT)	45±2°C	45±2°C	45±2°C	45±2°C	45±2°C	45±2°C	45±2°C	45±2°C	45±2°C
	Temp. coefficient of Pmax	-0.48 %/°C	-0.47 %/°C	-0.48 %/°C	-0.47 %/°C	-0.48 %/°C	-0.48 %/°C	-0.47 %/°C	-0.47 %/°C	-0.47 %/°C
	Temp. coefficient of Voc	-0.34 %/°C	-0.34 %/°C	-0.34 %/°C	-0.34 %/°C	-0.34 %/°C	-0.34 %/°C	-0.34 %/°C	-0.34 %/°C	-0.34 %/°C
	Temp. coefficient of Isc	0.037 %/°C	0.045 %/°C	0.037 %/°C	0.045 %/°C	0.037 %/°C	0.037 %/°C	0.045 %/°C	0.045 %/°C	0.045 %/°C

Figure C.2. Datasheet of SUNTECH STP050D-12MEA used in implementation